Surge Modeling and Control of Automotive Turbochargers

Master's thesis
performed in **Vehicular Systems**

by
Johan Bergström and Oskar Leufvén

Reg nr: LiTH-ISY-EX -- 07/3999 -- SE

June 14, 2007

Surge Modeling and Control of Automotive Turbochargers

Master's thesis

performed in **Vehicular Systems**,
Dept. of Electrical Engineering
at **Linköpings universitet**

by **Johan Bergström and Oskar Leufvén**

Reg nr: LiTH-ISY-EX -- 07/3999 -- SE

Supervisor: **Associate Professor Lars Eriksson**
          Linköpings Universitet

Examiner: **Associate Professor Lars Eriksson**
          Linköpings Universitet

Linköping, June 14, 2007

Avdelning, Institution Division, Department Vehicular Systems, ISY Dept. of Electrical Engineering Linköpings Universitet 581 83 Linköping		**Datum** Date June 08, 2007

Titel	Surgemodellering och reglering av fordonsturbo
Title	Surge Modeling and Control of Automotive Turbochargers
Författare Author	Johan Bergström and Oskar Leufvén

Sammanfattning
Abstract

Mean Value Engine Modeling (MVEM) is used to make engine control development less expensive. With more and more cars equipped with turbocharged engines good turbo MVEM models are needed. A turbocharger consists of two major parts: turbine and compressor. Whereas the turbine is relatively durable, there exist phenomenons on the compressor that can destroy the turbocharger. One of these is surge.

Several compressor models are developed in this thesis. Methods to determine the compressor model parameters are proposed and discussed both for the stable operating range as well as for the surge region of a compressor map. For the stationary region methods to automatically parameterize the compressor model are developed. For the unstable surge region methods to get good agreement for desired surge properties are discussed. The parameter sensitivity of the different surge properties is also discussed. A validation of the compressor model shows that it gives good agreement to data, both for the stationary region as well as the surge region.

Different open loop and closed loop controllers as well as different performance variables are developed and discussed. A benchmark is developed, based on a measured vehicle acceleration, and the control approaches are compared using this benchmark. The best controller is found to be a open loop controller based on throttle and surge valve mass flow.

Abstract

Mean Value Engine Modeling (MVEM) is used to make engine control development less expensive. With more and more cars equipped with turbocharged engines good turbo MVEM models are needed. A turbocharger consists of two major parts: turbine and compressor. Whereas the turbine is relatively durable, there exist phenomenons on the compressor that can destroy the turbocharger. One of these is surge.

Several compressor models are developed in this thesis. Methods to determine the compressor model parameters are proposed and discussed both for the stable operating range as well as for the surge region of a compressor map. For the stationary region methods to automatically parameterize the compressor model are developed. For the unstable surge region methods to get good agreement for desired surge properties are discussed. The parameter sensitivity of the different surge properties is also discussed. A validation of the compressor model shows that it gives good agreement to data, both for the stationary region as well as the surge region.

Different open loop and closed loop controllers as well as different performance variables are developed and discussed. A benchmark is developed, based on a measured vehicle acceleration, and the control approaches are compared using this benchmark. The best controller is found to be a open loop controller based on throttle and surge valve mass flow.

Keywords: Compressor, Mean Value Engine Modeling, Surge control, Surge line, Surge valve

Preface

This thesis is written for readers with good knowledge in control theory and mean value engine modeling (MVEM). The readers are expected to have acquired knowledge in spark ignited (SI) automotive engines through a course like "TSFS05 Vehicular systems" given at Linköpings universitet or similar. Furthermore it is recommended that the reader have read the Ph.D thesis "Air Charge Estimation in Turbocharged Spark Ignition Engines" by Per Andersson (2005). Since the Simulink MVEM models developed are based on the Simulink SI MVEM model developed, tuned and validated in Per Andersson´s Ph.D thesis.

Acknowledgment

We want to thank our supervisor Lars "Lasse" Eriksson at Vehicular Systems, for making this thesis possible and for his great support and insightful discussions. We would also like to thank Per Andersson, Fredrik Lindström and Johannes Andersen at GM-Powertrain, Sweden AB for showing interest in our work. Then we thank the opponents, Erik Andersson and Per Brännström, for their valuable feedback and comments. We would also like to thank Martin Gunnarsson for all his help with the computer system and Per Öberg for acting as a mailman. We are also thankful to the rest of the group at Vehicular Systems for interesting coffee breaks and master thesis student Fredrik Nilsson for always asking "Are you done yet?".

Contents

Chapter 1

Introduction, problem and outline

1.1   Introduction

From being exclusively for sports and performance cars, turbochargers are now a common thing, even in ordinary family cars. Ever increasing fuel prices and focus on the environment have forced the automotive industry from using large bigbore engines to using the advantages of downsized and turbocharged engines instead.

A turbocharger consists essentially of a turbine and a compressor. A compressor is essentially a fluid pump and share the same phenomenons as a pump. One such phenomenons is surge, which is highly unwanted. This is because surge is dangerous for the compressor. If an automotive turbocharger is driven in deep surge cycles for too long the turbo charger will break down. An effective fail safe method for avoiding surge is implemented in today's production cars. However, in ensuring safety in all cases, this method wastes much of the valuable pressurized air.

The goal with this thesis is to investigate the surge phenomenon and, with more knowledge about the phenomenon, to construct better controllers. Different control strategies that avoid surge and save as much pressure as possible are proposed and compared. The benefits of bigger, better and more expensive actuators are discussed. But to be able to investigate different control strategies a surge capable compressor model has to be developed first. This compressor model is implemented as part of a full turbocharged spark ignited engine Simulink model, see figure 1.1. For more information about the Simulink models a good start is to study Appendix A. For Mean Value Engine Modeling, (MVEM), and the original Simulink model it is recommended to study [1, 5, 6].

The question to be answered is if there are ways to increase the perfor-

mance of the engine with a more advanced controller? If it is so, could more
expensive actuators help even further? Only centrifugal automotive turbo-
chargers are investigated and described in the thesis. Most of the results
would probably apply for other turbochargers of approximately the same size
but this is not investigated.
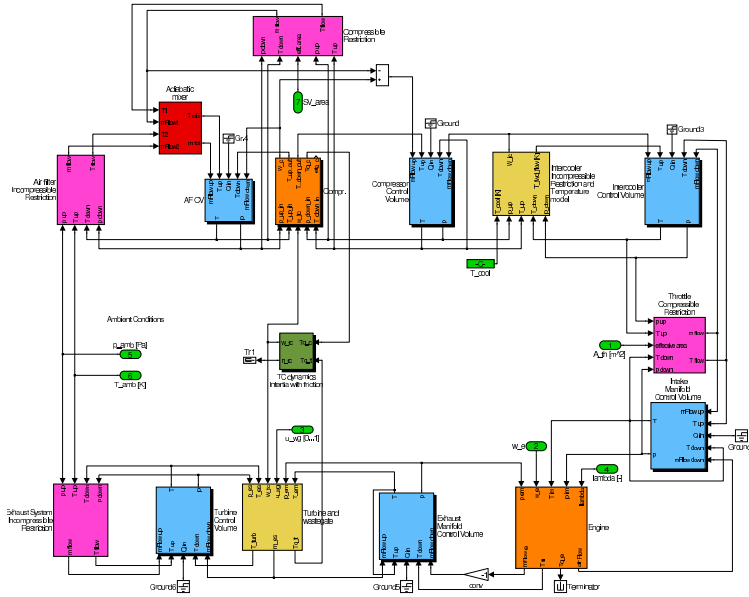
Figure 1.1: Engine model with a surge capable compressor model incorpo-
rated. The mass flow goes through (in order): air filter (upper left corner),
compressor, intercooler, throttle, intake manifold, cylinder(s), exhaust mani-
fold, turbine and exhaust system (lower left corner). These different com-
ponents are interconnected with control volumes between. The turbocharger
shaft is seen between the compressor and the turbine. The surge valve is seen
above the compressor block.

1.2   Problem

The problems to be investigated in this thesis are twofold

- Can methods be found to parameterize a surge capable compressor
  model. How good will the surge representation be? How sensitive
  is the model to its parameters?

- Can the performance of a modern turbocharged automotive engine be increased? Are there any performance gains from having more expensive control systems and actuators?

These two problems are the base for chapters 3 and 4, and chapters 4 and 5 respectively.

1.3 Outline

A stationary compressor model is presented in chapter 2. When the stationary performance is satisfactory the model is expanded to include even the unstable surge region of the compressor map. This is done in chapter 3. In chapter 4, different control approaches are presented. Different performance variables are also discussed in this chapter. Chapter 5 contains a comparison of the controller performances for a specific test case. The test case represents an acceleration with a normal gear change which is one of the most common ways of causing surge. Future work proposals are given in chapter 6. The thesis is summarized in chapter 7 and the conclusions are also presented.

1.4 Definitions

Throughout this thesis some terms are used to make the text easier to read. These are as follows:

- **Upstream and downstream:** The entire engine model acts as a "river" for the fluid. A component that gives mass to another component, during normal flow direction, is therefore said to be upstream.

- **Control volume:** A control volume is a representation of a physical volume. The tubes and pipes of an engine, the air filter box and intake manifold are examples of control volumes.

- **Pressure ratio:** The pressure ratio is defined as the pressure quotient between the pressure in a downstream control volume through the pressures in a upstream control volume (e.g. $\Pi_c = \frac{p_c}{p_{af}}$).

- **Reversed mass flow:** When the mass flow does not follow the normal order from an upstream to a downstream control volume, the mass flow is said to be reversed. This occurs during parts of a surge cycle.

The nomenclature used in the thesis is presented in Appendix B.

Chapter 2

Compressor models for stationary performance

In this chapter a compressor model with satisfactory stationary performance is presented. The models also describe the surge region of the compressor map but the estimation and validation of this region is presented in chapter 3. First the data used to estimate and validate the stationary performance is presented. This is followed by a description of the different parts that make up a compressor model and finally a validation of the chosen compressor model is made.

2.1 Stationary estimation and validation data

For this thesis, map data was given for four different compressors. All four maps consist of pressure, mass flow and efficiency in points along a number of lines of equal shaft speed. The values in each point are taken after a long period of time so that any system dynamics have stabilized. In the graphical representation of a compressor map the points of equal shaft speed are often connected forming (iso-)speed lines. The entire map of speed lines is sometimes referred to as the compressor characteristic. The efficiency points are also often connected, forming contours of equal efficiency. For the surge test rig compressor, stationary data for different operating points was also available. This data differs from the map data in that it was not a time averaged mean value but signals varying with time. The data also contained temperatures and other signals.

2.1.1 SAE corrections and corrected variables

The maps making up different compressor characteristics and isoefficiency contours are almost always given in terms of corrected quantities. This is

because by correcting the data and supplying the correction factors with the map, the characteristics can be calculated for different surrounding temperatures and pressures. The compressor maps can be corrected to any temperatures and pressures but the SAE (Society of Automobile Engineers) corrections [12] are commonly used. Models constructed from corrected map data must use scaled variables as input to be useful. In most compressor models both the efficiency and the pressure build up models use SAE corrected map data and both must therefore have this scaling of the appropriate input signals. The equations for doing this are

$$
\begin{cases}
N_{corr} & = \frac{N}{\sqrt{\theta}} \\
W_{corr} & = \frac{W\sqrt{\theta}}{\delta} \\
\theta & = \frac{T}{T_{std}} \\
\delta & = \frac{p}{p_{std}}
\end{cases}
\tag{2.1}
$$

The equations come from [6]. The temperature T_{std} and the pressure p_{std} are the correction temperature and pressure supplied with the data. For the other variables and subscripts see Appendix B.

2.2 Stationary compressor modeling and parameter estimation

The equations forming the compressor sub models will be described in this section. The compressor model is based on the compressor model equations originally developed by Moore-Greitzer. A good summary of the equations are given in [6]. The compressor model is divided into five sub models describing: temperature, torque, shaft dynamics, efficiency and pressure build up. For an overview of the compressor model developed see figure A.4.

2.2.1 Commonly used Moore-Greitzer sub models

Some of the compressor's sub models are commonly used independently of the different efficiency and pressure build up models discussed later. These sub models are presented here together with a brief parameter sensitivity investigation.

Temperature T_c

The temperature sub model describes how the compressor temperature depends on efficiency, pressure ratio and temperature of the upstream and downstream control volume. There are two different temperature models depending on whether the mass flow is reversed or not. In a normal operating point,

with positive compressor mass flow, the temperature going to the control volume downstream the compressor is calculated according to

$$T_c = T_{af} \cdot \left(\frac{\Pi_c^{\frac{\gamma-1}{\gamma}} - 1}{\eta_c} + 1 \right) \tag{2.2}$$

This equation comes from [1, 6]. For the case of reversed, surging, mass flow the temperature of the flow going back into the upstream control volume is

$$T_{af} = T_c \left(1 - (1 - (\frac{1}{\Pi_c})^{\frac{\gamma-1}{\gamma}})\eta_c \right) \tag{2.3}$$

This is the same equation as used by the turbine sub model in the original MVEM model developed in [1].

Torque Tq_c

The compressor torque describes how much torque the compressor demands from the turbo shaft to produce the mass flow. When the compressor is driven with a reversed mass flow the compressor is acting as a turbine and thus converting kinetic energy in the flow into an accelerating torque. This is seen in the torque equation where $T_c > T_{af}$ in every case of interest in this thesis and $N_{tc} > 0$. So when there is a change of sign in W_c the consumed torque changes sign.

$$Tq_c = \frac{30}{\pi} \frac{(T_c - T_{af}) \cdot c_p \cdot W_c}{N_{tc}} \tag{2.4}$$

The equation comes from [1] with $\omega_{tc} = \frac{\pi}{30} N_{tc}$.

Turbo shaft dynamics

The rotational speed of the shaft connecting the compressor impeller and the turbine is modeled using the equations proposed by [1]. The equation follows from Newtons second law for a rotating system.

$$\frac{d(N_{tc}\frac{\pi}{30})}{dt} = \frac{d\omega_{tc}}{dt} = \frac{1}{J_{tc}}(Tq_t - Tq_c - Tq_{tc,friction}) \tag{2.5}$$

J_{tc} is the shaft inertia including the turbine and compressor impeller. The turbine torque Tq_t and the shaft friction torque $Tq_{tc,friction}$ are given in the MVEM model.

Compressor mass flow W_c

The compressor mass flow equation is one of the most important parts of the surge capable compressor model developed. Given the compressor pressure

build up, $\hat{p}_c$, and the pressure in the downstream control volume, p_c, the compressor mass flow, W_c, is determined

$$\frac{dW_c}{dt} = \frac{\pi D_c^2}{4L_c} \cdot (\hat{p}_c - p_c) \tag{2.6}$$

The Moore-Greitzer models were first developed for axial compressors [8, 13] and the acceleration of mass is said to occur in a plug having the size, diameter and length, of the axial compressor. For a centrifugal compressor this length is hard to estimate. It could be seen as an idealized length of the compressor convolute. Even the diameter is hard to assess when looking at a centrifugal compressor since the convolute does not have a constant diameter.

The compressor inlet diameter is therefore used as D_c in this thesis, since it is easy to measure. The compressor or duct length, L_c, is considered a tuning parameter.

2.2.2 Efficiency

In this section two different compressor efficiency sub models will be described. The compressor efficiency η_c is modeled from surrounding pressures, temperatures, mass flow and given compressor parameters. η_c describes how well the compressor builds up pressure compared to increasing the fluid temperature. The definition of η_c is according to [6]

$$\eta_c = \frac{Power\ required\ by\ an\ ideal\ process}{Actual\ power\ consumed}$$

The isentropic process, which states that the entropy of the system remains constant [14], is said to be ideal. This means that there is no transfer of heat from the fluid to or from the surroundings. Thus, the η_c definition becomes

$$\eta_c = \frac{\Pi_c^{\frac{\gamma-1}{\gamma}} - 1}{\frac{T_c}{T_{af}} - 1} \tag{2.7}$$

6 parameter efficiency model

An efficiency model using six parameters is presented in [1], or slightly different in [6].

$$\begin{cases} \chi &= \begin{bmatrix} W_{c,\ corr} - W_{c_{\eta_{max}},\ corr} \\ 1 + \sqrt{\Pi_c - 1} - \Pi_{c_{\eta_{max}}} \end{bmatrix} \\ Q &= \begin{bmatrix} Q_{1,1} & Q_{1,2} \\ Q_{2,1} & Q_{2,2} \end{bmatrix}, Q_{1,2} = Q_{2,1} \\ \eta_c &= \eta_{c_{max}} - \chi^T \cdot Q \cdot \chi \end{cases} \tag{2.8}$$

The corrected quantities of the equations are calculated using the SAE corrections presented in section 2.1.1. Using this model, two different approaches

can be used depending on whether the three parameters $W_{c_{\eta_{max}},corr}$, $\Pi_{c_{\eta_{max}}}$ and $\eta_{c_{max}}$ are given or not.

Assuming that none are supplied by the manufacurer, all parameters can be estimated using the MATLAB function $lsqcurvefit$. This MATLAB function is sensitive to initial values of the parameters to be estimated. Depending on the initial values the estimation might, according to [1], terminate in several local minima and thus needs manual adjustments of the initial values. Therefore a loop is produced that uses a displaced normal distribution for these parameter's initial values. The center of the distribution is placed using intuition for the parameters. For example the $\eta_{c_{max}}$-parameter would be in the range $[0.5 \cdots 0.9]$. By looping through a large number of initial values and comparing the estimations a trend can be seen and the parameters are taken from where *lsqcurvefit* gives the largest number of estimations. For example if the estimation of the $\eta_{c,max}$-parameter would produce estimations in the range $[0.1 \cdots 1.2]$ with the majority of the estimations give 0.85, this value is used. The advantage is that no parameters are needed from the manufacturer. A disadvantage is that an intuitive feeling to get the initial values right is required.

Assuming that the three parameters ($W_{c_{\eta_{max}},corr}$, $\Pi_{c_{\eta_{max}}}$ and $\eta_{c_{max}}$) are supplied by the compressor manufacturer, there are only the three $Q_{i,j}$-parameters to estimate. This is accomplished using the MATLAB function for solving least squares problems. One advantage over the previous model is that there are only three parameters to estimate. The problem fo the initial values for the estimation does not exist either. The disadvantage is that parameters from the compressor manufacturer are needed. Using this model an efficiency map would look similar to figure 2.1.

The influence of the model parameters

To get a feeling for the different parameters used in the η_c-model their influence is examined here. To study their individual influence they are individually raised and the resulting efficiency contours are plotted. To better illustrate the different influences lesser efficiency lines are plotted than in figure 2.1. The results are shown in figure 2.2.

9 parameter efficiency model

Another efficiency model developed by Olof Erlandsson in [7] was also implemented and tested with a positive result. The equations for this model are

$$
\begin{cases}
\eta_c &= D_1 \cdot W_c^2 + D_2 \cdot W_c + D_3 \\
W_{c_{\eta_{max}}}(w_{tc}) &= \frac{-D_2}{2 \cdot D_1} \\
\eta_{max}(w_{tc}) &= D_1 \cdot W_{c_{\eta_{max}}}(w_{tc})^2 + D_2 \cdot W_{c_{\eta_{max}}}(w_{tc}) + D_3 \\
A_\eta(w_{tc}) &= D_1
\end{cases}
$$

$$(2.9)$$
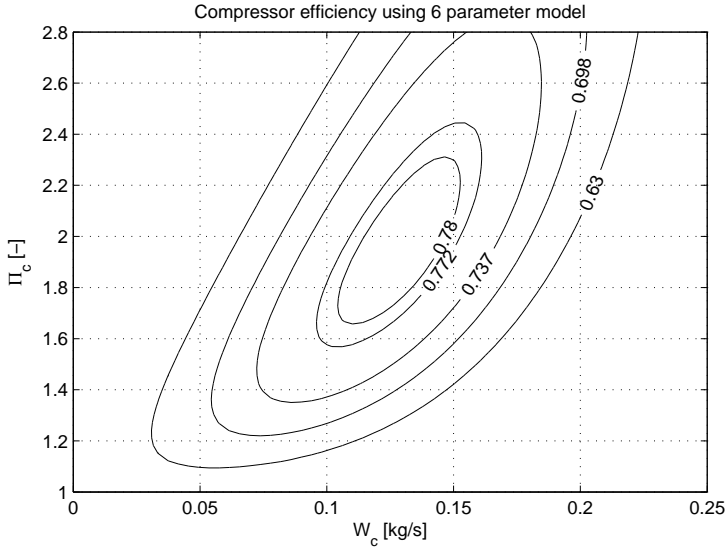
Figure 2.1: η_c using the 6 parameter model. Seen in the figure are the efficiency lines for selected values of efficiency. On the x-axis is the mass flow, on the y-axis the pressure ratio.
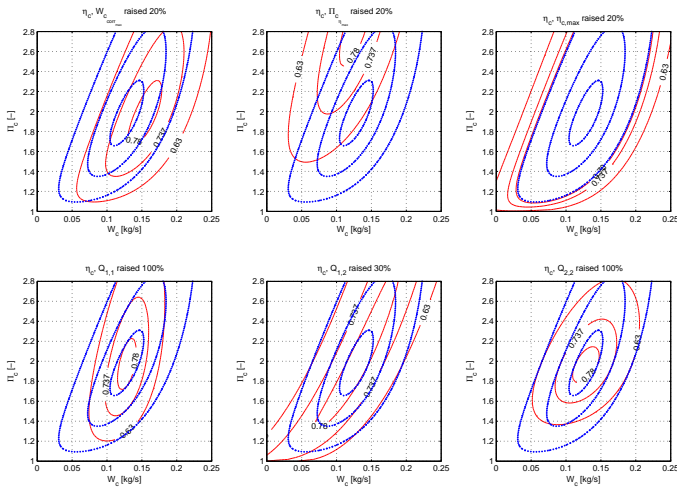
Figure 2.2: η_c dependency of different model parameters. Solid lines are efficiency of the unaltered model and dashed dotted are those with individual model parameters raised.

These are rewritten to

$$
\begin{cases}
\eta_c & = D_1(N_{tc}) \cdot W_c^2 + D_2(N_{tc}) \cdot W_c + D_3(N_{tc}) \\
D_1(N_{tc}) & = A_\eta(N_{tc}) \\
D_2(N_{tc}) & = -2 \cdot A_\eta(N_{tc}) \cdot W_{c_{\eta_{max}}}(N_{tc}) \\
D_3(N_{tc}) & = \eta_{max}(N_{tc}) + A_\eta(N_{tc}) \cdot W_{c_{\eta_{max}}}^2(N_{tc})
\end{cases}
$$

The three functions that appear in the right hand side of the equations are three second order polynomials in (corrected) shaft speed. A_η is called the second-degree coefficient, $W_{c_{\eta_{max}}}$ is the mass flow at maximum efficiency of each speed line and η_{max} is the maximum efficiency of the speed line. The coefficients of both the $W_{c_{\eta_{max}}}$ and the η_{max} polynomials are calculated using the method of least squares. The coefficients of the A_η polynomial are calculated using the MATLAB function *lsqcurvefit*. There are a total of 9 parameters to estimate, three for each polynomial. A general figure of the resulting efficiency is shown in figure 2.3.
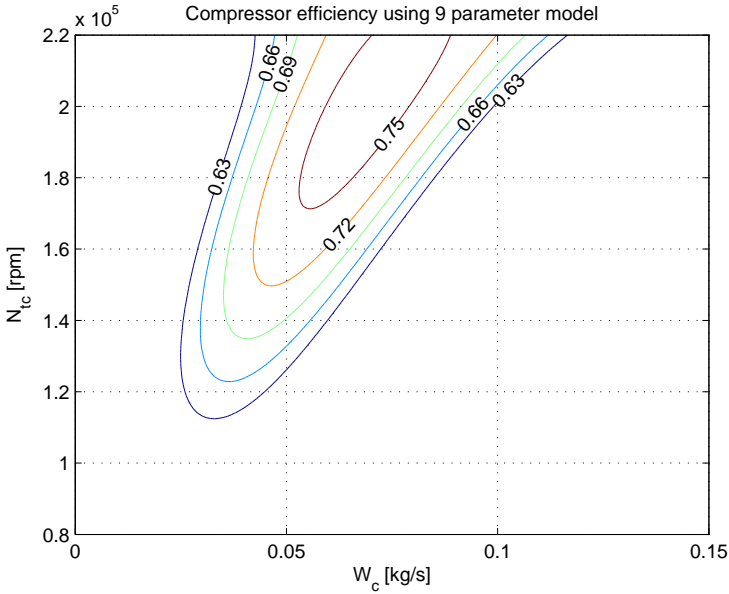
Figure 2.3: η_c modeled with the 9 parameter model. This model uses an efficiency as a function of shaft speed and mass flow. **Note**: Y-axis different to a normal compressor map!

Choice of efficiency model

A comparison plot of the different efficiency models is shown in figure 2.4. The figure shows that the 9 parameter model has larger mean error as well as standard deviation. The 6 parameter model is also more intuitive to work with since it uses the normal compressor map axes. The need for lesser parameters also makes it a more attractive model to use. For the following part of the thesis the 6 parameter model will be used.
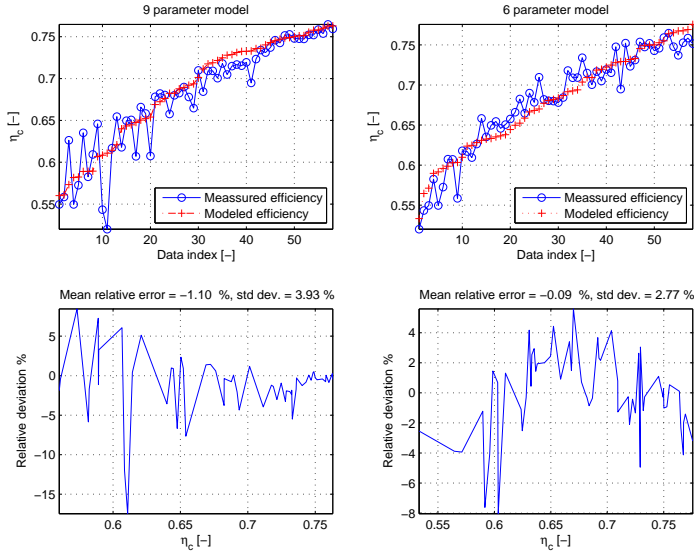
Figure 2.4: Comparison of the two different efficiency models. The 6 parameter model shows a smaller mean error as well as smaller standard deviation.

2.2.3 Pressure build up

The pressure build up that the compressor can produce is often shown as lines of constant shaft speed in graphical representations of compressor maps. These lines show how pressure build up and mass flow are connected (for different speed lines). There are different ways to form these lines. In the following three paragraphs different methods will be discussed. The stationary part of a compressor map is said to be between a region called choke and a surge line. For a description of the surge line and choke see chapter 3.

Moore Greitzer pressure build up

The model for compressor pressure build up by Moore Greitzer is based on dimensionless normalized air mass flow, Φ_c and the headparameter, $\Psi_c = f_{\Psi_c}(\Phi_c)$. The pressure build up, $\hat{p}_c$, is then calculated as a function of Ψ_c, shaft speed, air temperature and pressure

$$\begin{cases} \Phi_c & = \frac{R_a T_{af}}{N_{tc} D_c^3 p_{af}} \cdot W_c \\ \Psi_c & = f_{\Psi_c}(\Phi_c) \\ \hat{p}_c & = \left(\frac{1}{2} \frac{U_c^2 \Psi_c}{T_{af} \cdot c_p} + 1 \right)^{\frac{\gamma}{\gamma-1}} \cdot p_{af} \end{cases} \tag{2.10}$$

When estimating and forming the shape of the $f_{\Psi_c}(\Phi_c)$-function the measured compressor map has to be transformed into dimensionless parameters. This is done for the mass flow with the help of the first equation (2.10) and by using an equation for the head parameter according to

$$\Psi_c = c_p T_{af} \frac{\Pi_c^{\frac{\gamma-1}{\gamma}} - 1}{\frac{1}{2} U_c^2} \tag{2.11}$$

This equation comes from [1, 6] and is a component of the More-Greitzer compressor model. Through dimensionless numbers a few data points and measurements can be enough to describe the compressor in different conditions and combinations [6]. A compressor model using dimensionless numbers does not have to use the corrected variables described in 2.1.1.

   Head parameter, f_{Ψ_c}, functions
 To get a good behavior several approaches for the relationsip between Φ_c and Ψ_c have been modeled. The models are tuned so they have a minimum at $\Phi_c=0$ and a maximum at the surge line [6]. Further on is the derivative $\frac{d\Psi_c}{d\Phi_c}$ for $\Phi_c = 0$ supposed to be 0, meaning the Φ_c^1-coefficient of the polynomials has to be 0. This is because there is no pressure build up at zero mass flow independent of shaft speed. The general polynomial thus becomes

$$f_{\Psi_c}(\Phi_c) = a_n \Phi_c^{(n)} + \cdots + a_2 \Phi_c^2 + a_1 \tag{2.12}$$

The most commonly used order of the polynomial is 3 but higher orders could be used. The different models are described in the following.
   Three parameter third order polynomial model
The first and perhaps simplest approach is that a single polynomial for the entire Φ_c-range is chosen to describe the relationship between Φ_c and Ψ_c.

$$f_{\Psi_c}(\Phi) = c_3 \Phi_c^3 + a_2 \Phi_c^2 + a_1$$

The parameters are calculated using the method of least squares for the given map data.The advantage with a three parameter polynomial is that it consists of just three parameters to decide upon, and this makes it easier to tune. Another advantage is that the model is continuous for all Φ_c. The disadvantage

is that there is not a lot of freedom to form the different speed lines which could lead to good performance for some speed lines and not for others.

Different polynomials for different Φ_c-ranges

This model uses two different polynomials for different Φ_c-ranges. Left of the surge line three parameters are used because of the demand for the Ψ_c-derivative at $\Phi=0$. For mass flows right of the surge line four parameters are being used. The polynomial itself is of third order on both sides.

$$f_{\Psi_c}(\Phi_c) = \begin{cases} a_4\Phi_c^3 + a_3\Phi_c^2 + a_2\Phi_c + a_1 & \Phi_c \geq c \\ a_7\Phi_c^3 + a_6\Phi_c^2 + a_5 & \Phi_c < c \end{cases}$$

The reason for having four parameters for $\Phi_c \geq c$ is that the agreement to measured data in the stationary compressor region can be made better. A disadvantage would be that there are more parameters to tune and it is also discontinuous at the chosen c.

Shaft speed dependent model

One problem with the previous models for Ψ_c is that the parameter a_i might be dependent on shaft speed of the compressor, N_{tc}. Models covering this are found in for example [10] or [2]. To study this the transformed map-data is again used. A polynomial of third order in Φ_c with the Φ_c^1-coefficient equal to 0 is also this time desired. The difference is that the least square calculations are done once for every speed line in the given map-data so that different a_i:s are obtained for every speed line. These a_i:s were then parameterized using polynomials in shaft speed. Two different models were, also taken in consideration here, to model the dependency. Both models used the same base formula,

$$f_{\Psi_c}(\Phi_c) = a_3\Phi_c^3 + a_2\Phi_c^2 + a_1$$

but the a_i:s were calculated differently. For the simplest model a cubic relationship was assigned

$$a_i = a_{i,4}N_{tc}^3 + a_{i,3}N_{tc}^2 + a_{i,2}N_{tc} + a_{i,1}$$

meaning a cubic polynomial for each Ψ_c-coefficient and in all 12 parameters to be estimated. For the more advanced model a a_i-model

$$a_i = a_{i,5}N_{tc}^4 + a_{i,4}N_{tc}^3 + a_{i,3}N_{tc}^2 + a_{i,2}N_{tc} + a_{i,1}$$

were used. No significant improvements were achieved using the fourth order polynomials and the third order polynomial model was judged good enough to manage the shaft speed dependency.

Bezier model

A Bezier curve is a parametric curve defined by a number of points. This is used as a model by defining start and end points of each speed line in a stationary compressor map as start and end points for a quadratic Bezier curve. The

third point, the mid point, is estimated using the method of least squares. Between the speed lines given by the compressor map an interpolation method between the Bezier points of closest speed lines is used. The quadratic Bezier curve equation is [14]

$$B(t) = (1 - t)^2 P_{start} + 2t(1 - t)P_{mid} + t^2 P_{end} \ \ t \in [0, 1] \qquad (2.13)$$

Different versions were evaluated. The first used a polynomial estimation for the t-function. This version is fast to simulate but does not show as good a fit as the next version. This is due to the need to parameterize the t-function.

The second version found the crossing between the Bezier-curve, with interpolated start-, mid-, and end values, and a line in the map with constant mass flow. This version is shown in figure 2.5 together with circles representing the used map data. This version shows the best fit to the compressor maps of all tested pressure build up models. It does not use a parameterization of the t-function. Instead, it numerically finds the crossing between the current mass flow line and the Bezier curve. This is done once in every step of simulation causing the simulation times to increase significantly.

Even different versions with inter- and extrapolation between a max speed line given by a Bezier curve and the rest of the map constructed from a $\Psi_c(\Phi_c)$-relationship were tested. The main advantage is that the good fit of the Bezier-curve can be used to get a good representation of the important max speed line. This is important because if the compressor shaft speed is higher than a specific value the risk of damaging the compressor increases.

In general, for all the Bezier models, the model has at least 3 points in pressure ratio and mass flow consuming 6 parameters for each speed line. The Bezier model also needs to be complemented with a model for mass flow to the left of the surge line. The implemented and tested version used around 100 parameters but showed good fit to the stationary compressor map data.

Ellipse model

The last developed compressor pressure build up model uses ellipses, or more specific superellipses, to form the speed lines. A superellipse is a generalization of the normal ellipse [14] and looks like

$$1 = \frac{(x - h)^n}{a^n} + \frac{(y - k)^n}{b^n}$$

An Ellipse model is presented in [6]. The difference is that the here developed model uses even the exponential of the ellipse equation as a parameter. The ellipse model here developed is based on a good representation of the approximated surge line. Therefore two polynomials are constructed for this line, one for surge mass flow, $W_{c,surge}$, and one for surge pressure build up ratio, $\hat{\Pi}_{c,surge}$. These are modeled as polynomials in turbo shaft speed according to

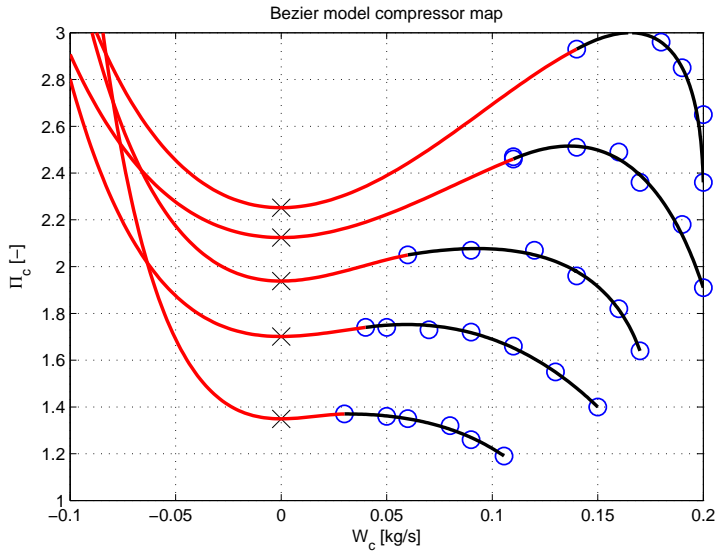$$W_{c,surge} = a_3 N_{tc,corr}^3 + a_2 N_{tc,corr}^2 + a_1 N_{tc,corr} + a_0 \qquad (2.14)$$

Figure 2.5: Bezier model with $\Psi_c(\Phi_c)$ left of the most left map point of each speed line. Pressure build up at zero mass flow is considered a design parameter (crosses). The fit to the given map data (circles) is good. The model captures even the highest speed line in a good way, which is something other pressure build up models do not.

$$\hat{\Pi}_{c,surge} = b_3 N_{tc,corr}^3 + b_2 N_{tc,corr}^2 + b_1 N_{tc,corr} + b_0 \qquad (2.15)$$

The parameters a_i, b_i are estimated using the method of least squares. This surge line representation is also, though slightly more restricted, presented in [6]. The differences are that the representation in [6] uses only cubic relationships for the surge line polynomials.

The compressor pressure build up is calculated as

$$\begin{cases} \hat{\Pi}_c &= \left(1 - \left(\frac{W_{c,corr}-W_{c,surge}}{c_1}\right)^{c_2}\right)^{\frac{1}{c_2}} (\hat{\Pi}_{c,surge} - 1) + 1 \\ \hat{p}_c &= \hat{\Pi}_c \cdot p_{af} \end{cases} \qquad (2.16)$$

The constants c_1, c_2 are estimated using the MATLAB-function *lsqcurvefit*. The constants are parameterized using polynomials in shaft speed according to

$$c_i = c_{i,3} N_{tc,corr}^3 + c_{i,2} N_{tc,corr}^2 + c_{c1} N_{tc,corr} + c_{i,0} \qquad (2.17)$$

A slightly better fit to the data could be achieved by not forcing zero derivative at the surge mass flow. Another method could be not to force the semimajor axis of the ellipse to have $\hat{\Pi}_c = 1$. Some freedom is lost if extrapolation outside the measured shaft speed is needed. This is done by forcing the surge line through ($W_{c,corr} = 0, \hat{\Pi}_c = 1$) for $N_{tc,corr} = 0$. Equations (2.14), (2.15) then become

$$W_{c,surge} = \hat{a}_3 N_{tc,corr}^3 + \hat{a}_2 N_{tc,corr}^2 + \hat{a}_1 N_{tc,corr} + 0 \qquad (2.18)$$

$$\hat{\Pi}_{c,surge} = \hat{b}_3 N_{tc,corr}^3 + \hat{b}_2 N_{tc,corr}^2 + \hat{b}_1 N_{tc,corr} + 1 \qquad (2.19)$$

For mass flows less than the surge mass flow of each speed line, a third order polynomial in $N_{tc,corr}$ and $W_{c,corr}$ is used. The different d_i in equation (2.20) are calculated so that the speed line has zero slope at zero mass flow, zero slope at the surge line and goes through the surge point of the current speed line. The pressure build up for zero mass flow is also parameterized as a polynomial in shaft speed. This gives the following equations

$$\begin{cases} \hat{\Pi}_{c,W_{c,corr}=0} &= d_n N_{tc,corr}^n + \cdots + d_0 \\ e_1 &= \hat{\Pi}_{c,W_{c,corr}=0}(N_{tc,corr}) \\ e_2 &= \frac{\hat{\Pi}_{c,surge}-a_1}{\frac{1}{3}W_{c,surge}^2} \\ e_3 &= \frac{-2a_2}{3W_{c,surge}} \\ \hat{\Pi}_c &= e_3 W_c^3 + e_2 W_c^2 + e_1 \end{cases} \qquad (2.20)$$

where the d_i:s are estimated using the method of least squares. The shape of this part of the speed line is thus given by the desired pressure build up ratio for zero mass flow. This is an important factor for the surge behavior and is thus taken as a design variable. A pressure build up map using the ellipse model is shown in figure 2.6
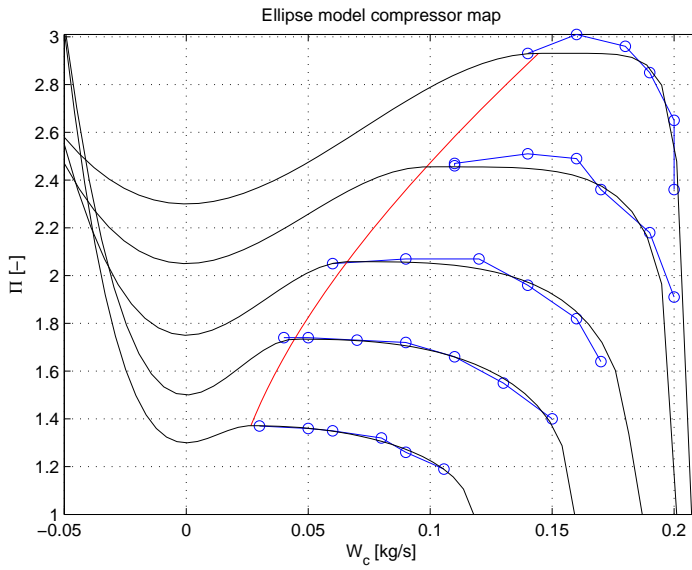
Figure 2.6: Ellipse model pressure build up map. The fit to the map data (circles) is good especially for lower speed lines. The approximated surge line is also shown.

Choice of pressure build up model

The pressure build up model chosen for the rest of this thesis is the Ellipse model since this has the best fit to the compressor map vs. parameter cost. The other models also show promising results and are certainly capable of producing a surge behavior. The Ellipse model is however easier to tune and intuitive to work with.

2.3   Stationary performance validation

Under this section a validation of the compressor model consisting of the chosen sub models is given. The section is divided into a sub model validation, first of the efficiency, then the pressure build up followed by a full compressor model validation.

2.3.1   Stationary efficiency validation

To validate the chosen efficiency model, different corrected maps were used and the modeled efficiency and measured data were compared. This is shown for two of the four available compressor maps. The validation plot for two of the compressors is shown in figure 2.7. Due to lack of data the same data has been used both for parameter estimation and validation. During normal operating ranges an automotive compressor is kept at high levels of efficiency. The deviation for $\eta_c \leq 0.60$ is therefore not of big interest. The parameter estimation is however done using all available η_c-points. A slightly better fit for higher efficiencies would be possible if the parameter estimation were done using only map points having higher η_c-values. This would probably be of more interest in an production application where the efficiency for map regions outside the desired is of lower interest. However, the objective of this thesis is to look at the compressor as a physical component. The efficiency for all possible operating points is, therefore, of interest.

2.3.2   Stationary pressure build up validation

The stationary part of the compressor map is modeled using the chosen pressure build up model (Ellipse). For two of the given compressor maps enough speed lines were available in the data to be able to use some of them to parameterize the model and the rest as validation data. The result is given in figure 2.8. This shows that the ellipse pressure build up model is a good choice. The fit to the data is better for lower shaft speeds than for higher. The relative error is lower for higher pressure ratios than for lower.
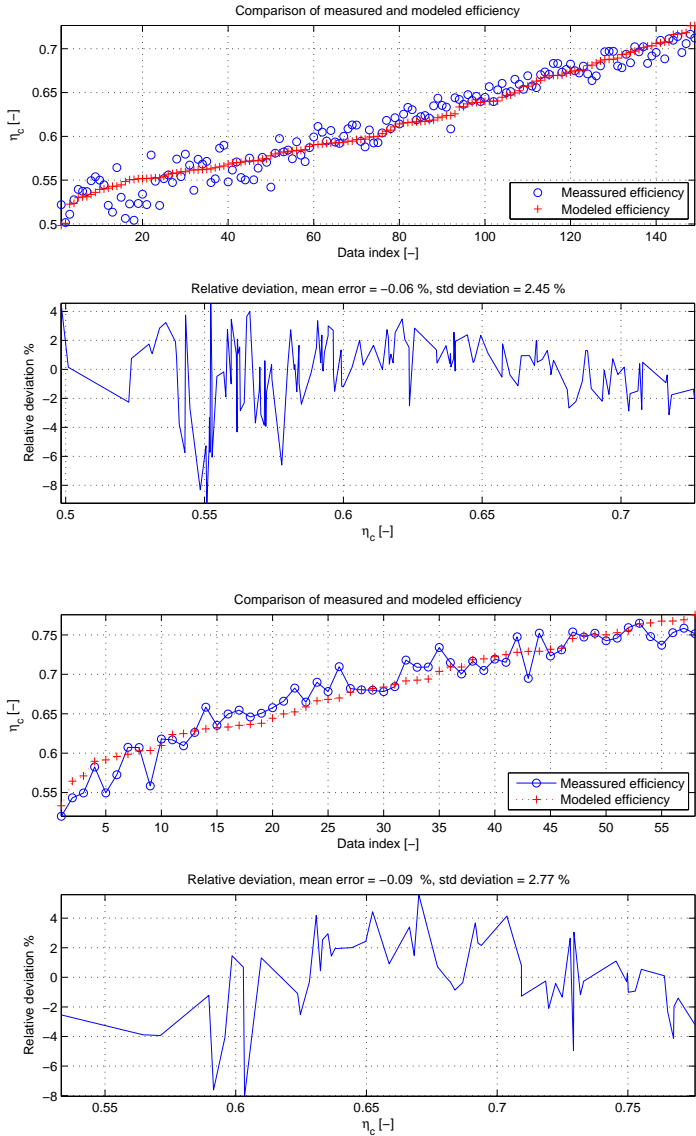
Figure 2.7: Validation of η_c. Circles represent measured data and plus modeled values. Shown is also the relative error with a mean relative error and standard deviation. The validation plots are for two different compressors. The normal operating point of an automotive compressor is at higher levels of efficiency ($\eta_c > 0.6$). The model also shows best performance higher efficiencies.
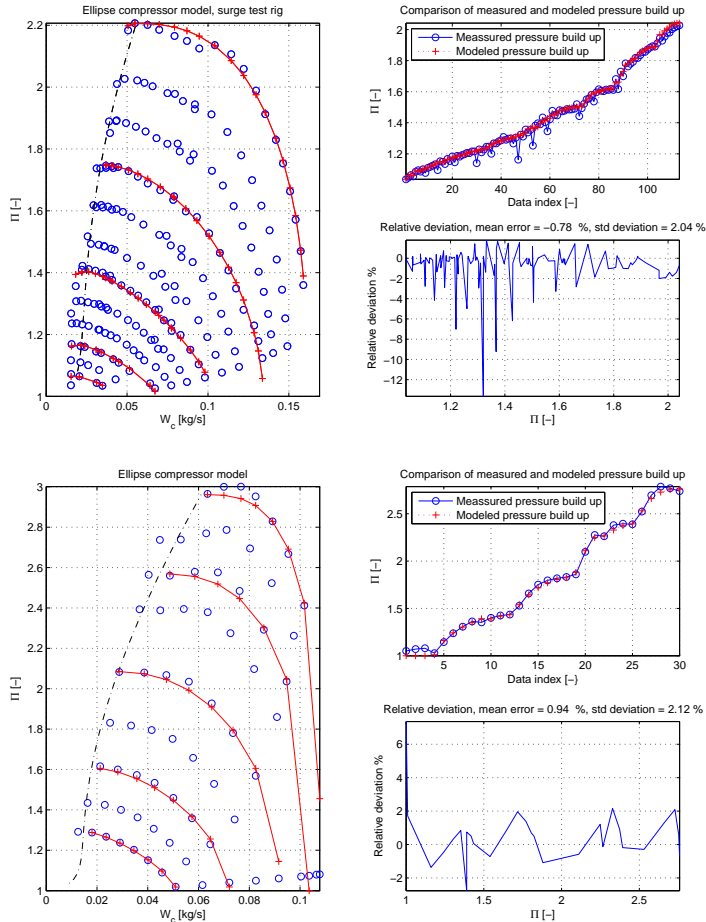
Figure 2.8: Validation of $\hat{\Pi}_c$. **Left:** Given data. Circles represents measured data and plus signed solid lines modeled values, also showing the speed lines used for parameterization. **Right:** Validation plots using the not marked speed lines of the left plot as validation data. For the validation data points left of the dashed dotted approximated surge line are ignored. Shown is the relative error with a mean relative error and standard deviation. The error is smaller for higher pressure ratios which is good because the surge line is at high pressure ratios on each speed line (see section 3.3.3). The $\hat{\Pi}_c$ denotes pressure build up ratio not to be mistaken for compressor pressure ratio Π_c because this denotes pressure ratio of the control volumes up- and downstream of the compressor.

2.3.3   Full stationary compressor model validation

The full compressor model validation is done using data from the surge test rig. The rig was run stationary for a long period of time at constant throttle angles. This data is collected under a normal run and the data is not corrected. Therefore the correction factors described in 2.1.1 have to be used for signals going into the efficiency and pressure build up models. This validation is done using the test rig Simulink model, see section A.3, where measured signals are used as input. The validation plot in figure 2.9 shows pressure build up and efficiency for two shaft speeds ($100.000\,[rpm]$, $120.000\,[rpm]$). The validation shows that the model agreement with data is good, but close to the surge line the compressor is sensitive even to small variations in pressure. This since the slope of the compressor characteristic is close to zero at this point. The data used is for operating points close to the surge line and the pressure difference between each data set is therefore not big. Better validation data would have operating points covering the entire compressor map, but the validation shows that the models have a good behavior close to surge. Some of the relative error in the efficiency can be reduced if lesser map efficiency points are used for parameterization, discussed in section 2.3.1.

2.4   Stationary performance summary

This chapter started with a presentation of the available data. A brief discussion of corrected variables and the correction equations were presented. The different sub models of a full surge capable compressor model are also described in this section. The implemented equations are presented in connection with the descriptions. The equations are valid for both the normal operating range as well as for the surge region of the compressor map. For some of the sub models different methods are tested and these methods are compared. A sub model and full model validation, for the normal operating region, is presented last in the chapter.

The developed compressor shows good agreement to measured data. The validation of the pressure build up, as well as the efficiency shows good agreement especially for lower shaft speeds. The agreement is better for higher values of Π_c and η_c. When the developed compressor model was run with time varying signals the average relative pressure build up error equaled zero. The relative efficiency error was smaller than 10%. The larger relative errors seen in the efficiency validation could be due to not stabilized temperatures of the time varying data.

The Bezier pressure build up shows the best fit for higher shaft speeds. The Bezier model can be used for high shaft speeds in combination with another pressure build up approach for lower shaft speeds. Interpolation is used between these pressure build up models.
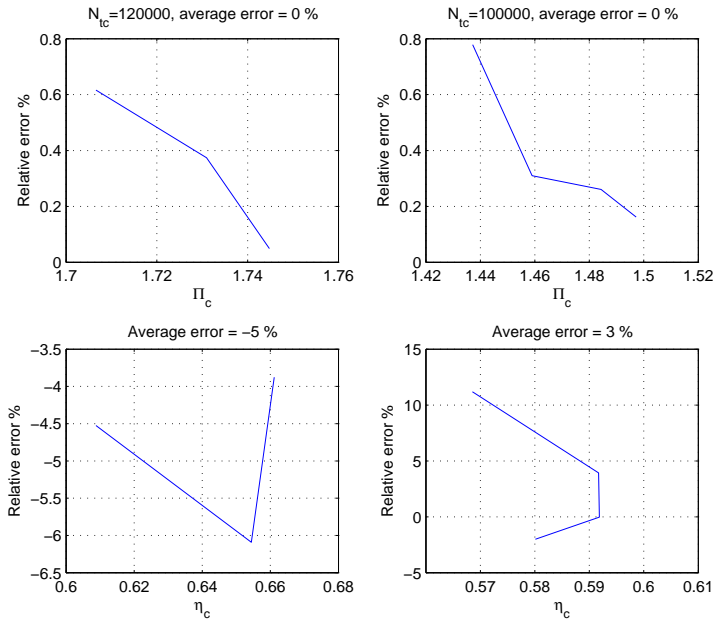
Figure 2.9: The figure shows the relative pressure build errors and efficiency errors for two shaft speeds. Due to lack of validation data only operating points close to each other were tested. The efficiency shows larger errors than the pressure ratio. The average relative error in pressure build up equals zero for both shaft speeds tested, but the compressor is sensitive to even small changes in pressure for operating points close to the surge line. The efficiency shows a larger error especially for some operating points. This can be due to the data being measured close to the surge line and some points might experience a mild surge behavior.

Chapter 3

Surge modeling and sensitivity

The phenomena to be studied in the thesis, surge, is investigated in this chapter. First, the available dynamic surge data will be described. This is followed by a presentation of surge and the properties of the surge cycles found in the surge data. Finally each property is described and how the property can be modeled is explained. The model discussion is done combined with a model parameter sensitivity analysis.

3.1 Dynamic estimation and validation data

Two different types of data is used in this chapter

- Compressor driven by a separate electric motor in a surge test rig/bench.

- Compressor as part of a turbocharger installed in an SI-engine (from the test bench at Vehicular Systems, ISY, LiTH, LiU)

These two differ in that a turbine driven compressor mounted in a real engine experiences a sudden drop in driving torque when the throttle closes, while a compressor in a surge test bench does not. This is because when the throttle closes, the engine can not consume as much air as before and to keep $\lambda = 1$ the amount of fuel injected is also reduced. This creates a drastic decrease in energy in the exhaust gases that the turbine can use and therefore the driving torque is reduced. This is not seen in a compressor test bench because a separate motor with a control system keeps the shaft speed constant. An example of data of the first type is given in figure 3.1 and of the second type in figure 3.2.
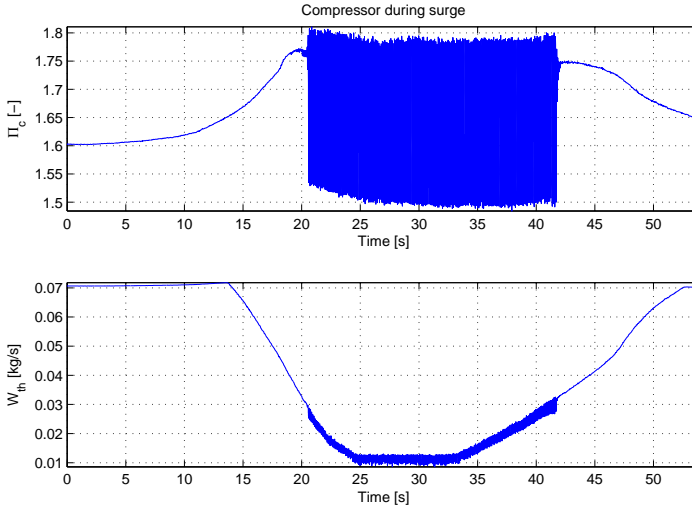
Figure 3.1: Example of surge data from the surge test bench showing compressor pressure ratio Π_c and throttle mass flow W_{th}. The compressor has been driven in surge for an extended period of time. It is questionable if a normal turbocharger also having a turbine and a full shaft would sustain this long period of surge. However, the test rig compressor does not have a turbine wheel. For a constant throttle mass flow the pressure dips are all of the same amplitude and share the same surge cycle time. The pressure oscillation amplitudes and cycle times are slightly different for different throttle mass flows even though N_{tc} is kept constant.
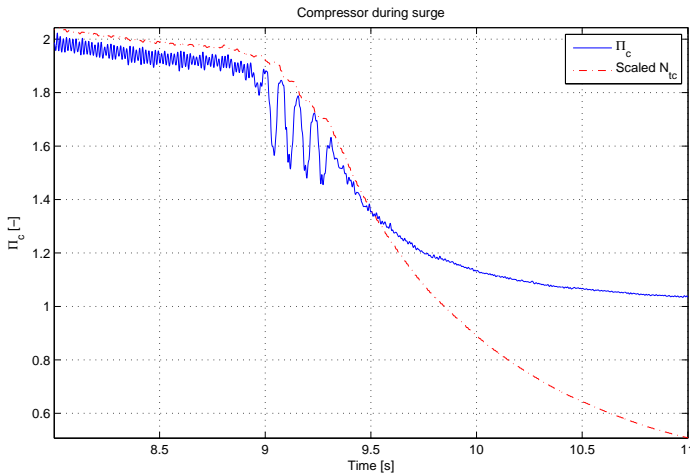

Figure 3.2: Example of surge data from the engine test bench at LiU showing compressor pressure ratio Π_c and (scaled) shaft speed N_{tc}. The figure shows four complete surge cycles. The different surge dip amplitudes can be seen as well as small deviation from the general trend in shaft speed. The data has been filtered.

3.2   Surge

The compressor map can be divided into three different regions. First there is the normal operating region in which the compressor normally works. This is mainly shown by the efficiency contours in the compressor map. To the lower right of the compressor map there is a region called choke. The compressor chokes when the quotient of mass flow and pressure is too large. These first two cases are not dangerous for the compressor, even though choke is often not desired. The last region of the compressor map is limited by the surge line. When the compressor travels beyond this line, surge will occur. This is because the compressor is unable to maintain flow lines and therefore the flow breaks down. This breakdown of flow lines causes uneven distributed load on the compressor blades and bearings [6]. When the flow breaks down completely, the highly pressurized air travels upstream, reversing the mass flow. The compressor now acts like a turbine. This upstream mass flow causes the pressure ratio to reduce until the compressor is able to again maintain positive mass flow. The pressure ratio then increases again and the compressor enters a new surge cycle, if no other changes are applied to the system.

The most common way to impose the risk of surge is to suddenly close the throttle of the intake manifold. This produces a sudden stop in throttle mass flow but the compressor wheel is spinning with such a speed that it continues to build up pressure. Such throttle closing occurs at every gear change. Other extreme ways to produce surge always involve sudden drops in demanded mass flow. This could be caused for example when an engine fails entirely and the cylinders stop consuming air. Another less extreme way would be if someone slips from the clutch pedal at high engine rpm:s or an automatic gearbox changes gear.

Surge is divided into three subgroups [15]

- **Mild surge:** No flow reversal and small oscillations in pressure.

- **Classic surge:** Low frequency oscillations with larger pressure oscillations.

- **Deep surge:** Reversal of the mass flow through the compressor.

The most interesting group, for the purpose of this thesis, is deep surge because this is the most dangerous case. The two subgroup case [6] is a generalization of the three, where the first two subgroups presented above together are called *mild surge*.

3.2.1   Surge properties

A surge cycle is characterized by different properties. In this section the following different surge properties are described

- **Surge pressure dip:** Every surge cycle has a specific pressure dip. If the cycles are continued without changing the operating point the pressure dip size prevails.

- **Surge cycle time:** When an operating point demand has caused surge, the surge cycles will continue with a specific cycle time until the demanded operating point is changed.

- **Surge temperature behavior:** The mass reversing through the compressor changes the temperature of the the upstream control volume.

- **Surge shaft speed variations:** The shaft speed of a freely rotating, not engine driven, compressor experiences variations during a surge cycle.

- **Where in the compressor map surge starts:** The points where surge starts on each speed line, form the surge line.

A surge cycle from the engine test bench at Linköpings University is shown in figure 3.3. The figure shows some of the surge properties.

Given these surge properties the need for information about the surge region is motivated. The different properties are investigated in the following sub sections.
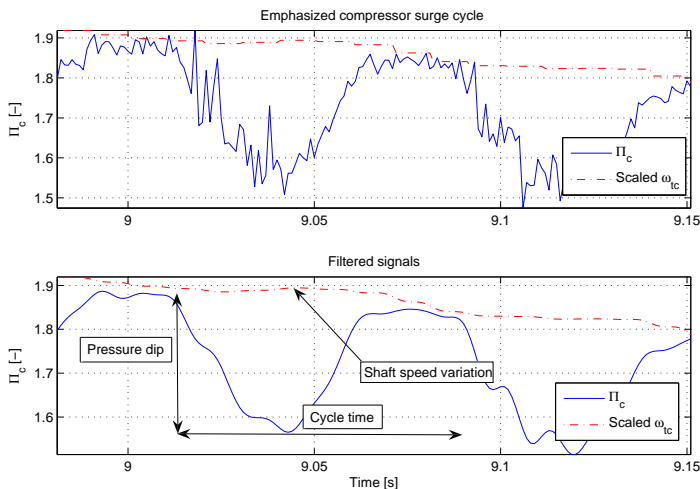

Figure 3.3: Measurement from the test cell engine during surge. The pressure dip, surge frequency and shaft speed variations are emphasized. The lower graph shows filtered data to easier separate the measurement noise from the signal. Both Π_c and N_{tc} are seen. In the lower graph some of the properties of a surge cycle are also marked.

3.3 Surge modeling

In this section, the surge side of the compressor model will be estimated and validated. The equations for the surge side, were presented in the previous chapter. The model parameter sensitivity will be investigated. Each surge property presented in the previous section will be discussed. Some of the surge properties share the same parameter sensitivity and are therefore investigated together.

3.3.1 Surge pressure dip and surge cycle time

The surge pressure dip and the surge cycle time property have much of the parameter sensitivity in common. The properties are described under separate paragraphs and these paragraphs are followed by a parameter sensitivity analysis common for both properties.

Surge pressure dip

Looking at the available surge data there is a clear pressure dip trend to be seen. The dip becomes increasingly larger for compression ratios. Studying the data from the surge test rig (figure 3.1), where the compressor has been driven in surge cycles for long periods of time and with constant shaft speed, the pressure dip is the same regardless of how long the surge has been in progress.

The pressure dips found in the different types of data sets available are presented in table 3.1 and 3.2. Table 3.1 shows how big the pressure drop during surge is, for a range of constant N_{tc}-values and different throttle closing speeds. It also shows how the surge cycle time varies. The surge rig data contains forced surge for long periods of time and the table therefore contains information from both one of the first surge cycles as well as from one of the last. The compressor is mounted in the surge test rig, effectively meaning that N_{tc} does not vary. The reason for the two different T_{cycle} for $N_{tc} = 120000 \, [rpm]$ is that the test bench geometries were changed to a larger compressor control volume (the tube downstream) for the larger time.

For the other surge data type the test bench in Vehicular Systems at LiU was used. The data contains two surge periods with 4 and 7 surge cycles respectively. During these surge periods N_{tc} as well as $\Delta\Pi_c$ varies. The initial (init) rotational speed and compressor pressure ratio are therefore presented along with each surge cycle's individual surge cycle time and pressure drop. Here, initial means where the pressure first starts to drop significantly. The first and last surge cycle of each surge period in the table differs slightly from the behavior of the cycles in between. The result is given in table 3.2.

N_{tc} [rpm]	$\Delta\Pi_c$ [−]	T_{cycle} [ms]	Comment
40.000	0.050	75	Fast thr., first cycles
40.000	0.048	70	Fast thr., last cycles
40.000	0.052	70	Slow thr., first cycles
40.000	0.046	70	Slow thr., last cycles
120.000	0.35	80	Fast thr., first cycles
120.000	0.32	81	Fast thr., last cycles
120.000	0.36	75	Medium thr., first cycles
120.000	0.36	80	Medium thr., last cycles
120.000	0.37	80	Ultraslow thr., first cycles
120.000	0.39	80	Ultraslow thr., last cycles
120.000	0.31	105	Fast thr., first cycles
120.000	0.30	106	Fast thr., last cycles
120.000	0.33	100	Slow thr., first cycles
120.000	0.36	110	Slow thr., last cycles

Table 3.1: $\Delta\Pi_c$ and T_{cycle} for the surge test rig with two different geometries. The bottom section of the table differs from the upper two in that a larger compressor control volume was used for these measurements. *First cycles* refers to values from one of the first cycles of the surge period and *last cycles* refers to one of the last cycles before the compressor was stabilized again. *Fast/Medium/Slow/Ultraslow* refers to how fast the throttle is closed.

#	$N_{tc,init}$ [rpm]	$\Pi_{c,init}$ [−]	$\Delta\Pi_c$ [−]	T_{cycle} [ms]
1	120000	1.880	0.310	78
2	116000	1.830	0.310	79
3	112000	1.750	0.210	77
4	108000	1.700	0.240	73
1	117000	1.840	0.250	80
2	114000	1.810	0.300	70
3	109000	1.730	0.260	80
4	105000	1.670	0.240	80
5	100000	1.620	0.230	70
6	96000	1.540	0.190	80
7	93000	1.500	0.180	70

Table 3.2: $\Delta\Pi_c$ and T_{cycle} from the engine test bench. The different $\Delta\Pi_c$ for different $N_{tc,init}$ are seen. Due to difficulties defining the exact start point of each surge cycle the values are rounded.

Surge cycle time

The reversed mass flow through the compressor will continue to grow until pressure build up, $\hat{p}_c$, exceeds the downstream pressure,p_c. Thus, the compressor characteristic for reversed (negative) mass flow determines how much the pressure downstream has to decrease until the compressor flow lines can be restored. The volume downstream of the compressor to the throttle and the flow characteristics of the components in between, determine how much mass flow that needs to be reversed to lower the downstream pressure sufficiently. When the downstream control volume pressure is decreased, the flow lines are restored.

Parameter estimation and sensitivity

The parameter estimation and sensitivity analysis is divided into two subgroups. The first investigates the effect of different control volume sizes, throttle mass flows, shaft speeds and compressor lengths. The second investigates the effect of different compressor characteristics for negative mass flow. These both groups are summarized at the end of this section.

   The parameters $V_{merged\ CV}$**,** W_{th}**,** N_{tc} **and** L_c
The compressor system is simplified by grouping the compressor control volume and intercooler control volume together, neglecting the pressure dip over the intercooler and assuming constant temperature in this merged control volume. The temperature rise caused by the compressor is also taken as a constant. The temperature in the merged control volume is taken as $330\,[K]$. This temperature comes from studying the temperature behavior of the developed Simulink MVEM model. Further on pressure and temperature upstream the compressor are said to be according to the SAE standard [12]. This means that no SAE corrections are required by the pressure build up model since $p = p_{std}$ and $T = T_{std}$ in equation (2.1). The equations describing this simplified system become

$$\begin{cases} \frac{dW_c}{dt} & = \frac{\pi D_c^2}{4L_c}(\hat{p}_c - p_{merged\ CV}) \\ \frac{dm_{merged\ CV}}{dt} & = (W_c - W_{th}) \end{cases} \qquad (3.1)$$

where $\hat{p}_c = \hat{p}_c(N_{tc}, W_c)$ is calculated using the Ellipse pressure build up model presented in section 2.2.3. The ideal gas law is used for the merged compressor control volume pressure, $p_{merged\ CV} = \frac{m_{merged\ CV}RT_{merged\ CV}}{V_{merged\ CV}}$. The sizes of the different control volumes making up $V_{merged\ CV}$ are often easy to estimate using simple measurements. The time constants of a surge cycle is much smaller than the dynamics of the shaft and N_{tc} is therefore taken as a constant.

   Simulations conducted with this simplified system, using the geometries of the surge test rig, are shown in figure 3.4. The system is released from a stable operating point near choke. The throttle mass flow is then suddenly

reduced to a much smaller value and the effect of varying the parameters in
equations (3.1) is studied. Figure 3.4 shows that a lot of parameters affect the
surge cycle time, even in the case of this simplified system.

If the surge time of this simplified system is compared to those presented
last in table 3.1 they almost coincide. The simplified model is thus describ-
ing the surge frequency well. The largest uncertainty is the compressor/duct
length, L_c, since this is more or less a theoretical construction when using the
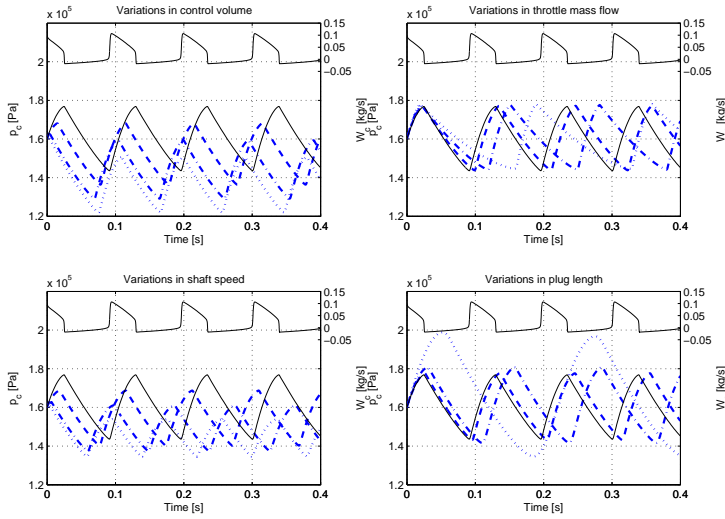Moore-Greitzer compressor model (see the discussions in section 2.2.1).

Figure 3.4: The effect on the surge cycle time and pressure dip from different
changes in the system. Solid lines show unaltered parameters from the surge
test rig for comparison purposes. Dashed, dashed dotted and dotted are sys-
tems with one parameter altered relative the original system. Upper left shows
variations in merged control volume and lower left variations in shaft speed.
These are varied to 85%, 90% and 95% of the original values of 5.83 $[L]$ and
120000 $[rpm]$ respectivly. Upper right shows variations in throttle mass flow
and lower right compressor (plug) length. These are varied to 20%, 50% and
80% of the original values of 0.02 $[kg/s]$ and 1 $[m]$ respectivly. The com-
pressor control volume pressure for the different parameters is shown as well
as the mass flow for the surge cycle of the original, unaltered system.

Using the information presented in figure 3.4 the surge rig Simulink model
is adjusted to predict the pressure dip and surge cycle time of the measured
data. When adjusting the parameters, a better fit to measured data is achieved
by altering the values for the merged control volume and the plug length.

The best fit values for the control volume size do not vary significantly for the tested surge cycles ($40000\,[rpm]$ and $120000\,[rpm]$) but the plug length shows dependency on rotational speed. The plug size that gives best fit to the surge cycles at $N_{tc} = 120000\,[rpm]$ is about 50% smaller then the one for $N_{tc} = 40000\,[rpm]$.

The resulting simulated compressor control volume pressure for $N_{tc} = 120000\,[rpm]$ is shown in figure 3.5. Inputs to the surge rig Simulink model used are measured signals and the pressure from the model is plotted together with the measured pressure. The Simulink model enters surge slightly later than the surge rig measurement and this time delay continues. The first surge cycle in the measured data also shows a slightly different pressure curve.
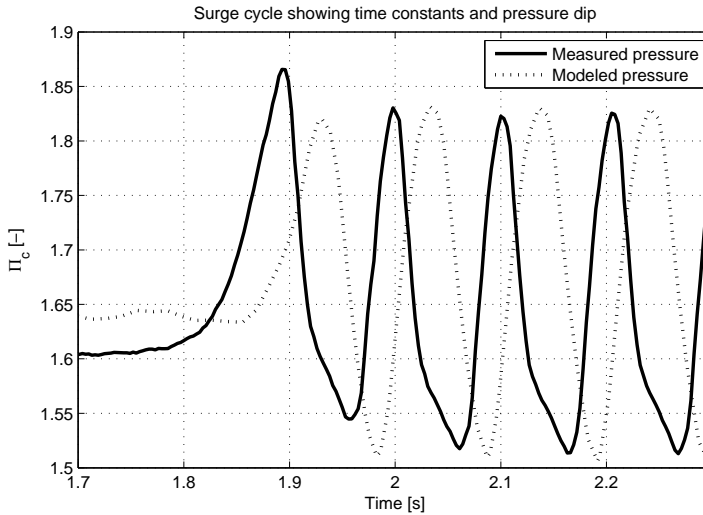

Figure 3.5: Measured (solid) and simulated (dashed) surge cycle pressure. To get a good model behavior the merged control volume had to be increased about 20% in size compared to the original size of $5.83\,[L]$. This could be caused by heat exchange to the surroundings in the measured data.

Speed line shape for negative mass flow

Since it is almost impossible to get manufacturer measurement for pressure build up outside of the normal operating region, it is of great interest to see the model sensitivity of these shapes. The Ellipse model models these speed lines as polynomials in corrected rotational speed and mass flow according to equation (2.20). Again, using the merged control volume model according to equations (3.1) simulations are conducted with the Ellipse pressure build up model and a modified Ellipse model. Both models were parameterized for the surge test rig compressor in the stationary region and used the same

shape of the speed lines down to zero mass flow. The difference is that at
mass flow less than zero the modified Ellipse model uses a constant value for
the pressure build up while the original uses a pressure build up according
to figure 2.6. This modification is rather drastic and the effects are clearly
visible in figure 3.6. The mass flow and pressure dip are much larger. The
reason for this is found in the mass flow equation

$$\frac{dW_c}{dt} = \frac{\pi D_c^2}{4L_c} \cdot (\hat{p}_c - p_{merged\ CV})$$

The mass flow will continue to decrease until $\hat{p}_c = p_{merged\ CV}$. With a con-
stant $\hat{p}_c$ for $W_c \leq 0$ it takes longer time to lower the downstream pressure
enough to fulfill this criterion. This means the mass flow will continue to
decrease for a longer period of time. The influence on T_{cycle} is a lot smaller
than the pressure and mass flow differences. This is because the control vol-
ume pressure, $p_{merged\ CV}$, is descending quickly when W_c is this negative.
The opposite is also true, $p_{merged\ CV}$ is increasing fast for large W_c.
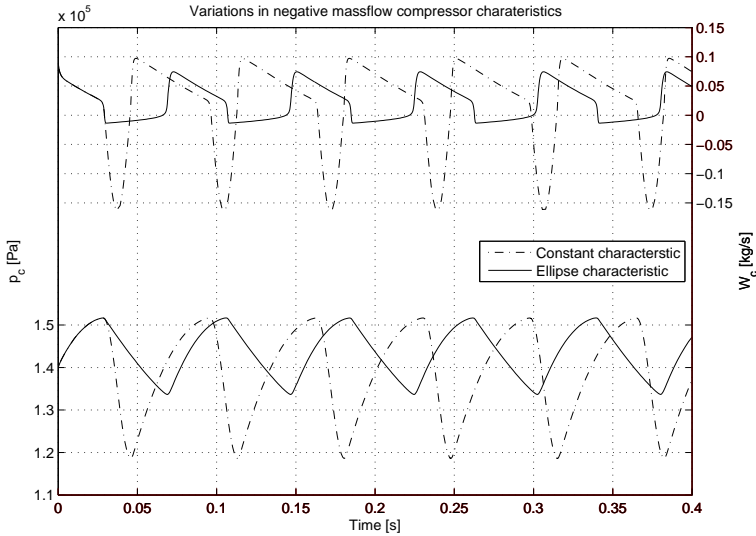
Figure 3.6: Solid lines represent a model using characteristics according to
figure 2.6 and dashed dotted lines a modified model with constant pressure
build up for negative mass flow. Both control volume pressure variations and
compressor mass flow variations are shown.

T_{cycle} and surge pressure dip parameter sensitivity summarized
The surge pressure dip is highly dependent on the compressor length L_c.
T_{cycle} shows a high dependency on control volume size. The compressor

characteristic for negative mass flow, in fact, affect both T_{cycle} and the pressure dip. However, it has the greatest affect on the amplitude of the mass flow variations. The throttle mass flow has minor effect on the cycle time and hardly any effect on the pressure dip.

Estimating the compressor characteristic for negative mass flow is done comparing the model output to the measured surge cycles of the surge test rig. Used as design parameter in the Ellipse pressure build up model is, among others, the pressure build up at zero mass flow. This value has great impact on how deep the pressure and mass flow dips get.

3.3.2 Surge temperature and shaft speed variations

Looking at the temperature equations (2.2), (2.3) and the torque equation (2.4), it is easy to see a connection. The torque consumed/produced by the compressor is highly dependent on the temperature changes and the direction of the mass flow. The measured data shows interesting shaft speed variations. This speed can vary due to two things; variations in produced torque (by the turbine) or variations in consumed torque (by the compressor or shaft friction). Due to their close connection they are investigated together.

Surge temperature

Looking at simulations, using the full SI MVEM model, the driving torque diminishes rather quickly when the throttle is closed but the shaft speed variations continues. An acceleration in shaft speed must then come from the compressor acting as a turbine for the reversed flow and thus takes energy from the fluid. The compressor torque is difficult to measure and is most often calculated from other measured signals. Even the surge temperature can be challenging to measure because of slow temperature sensors and heat losses to the surroundings.

Looking at the temperature measurements of the surge test rig when it is driven in surge for long periods of time, see figure 3.7, a general trend is seen. The temperature rise when the compressor enters surge is obvious. This is caused by heated pressurized mass going back through the compressor. The measured temperature shows a clear first order system behavior. A good approximation of the system time constant and final value can be obtained from the figure. Extending the graph for a longer period of surge by interpolation gives a final value for the temperature rise of about $55\ [K]$. The time constant is found to be about $6\ [s]$. The time constant is partly due to the relative slow response of the temperature sensors used.

Once the temperature is stabilized the final value of the system shows the air temperature of the average mass flow. This mass flow consists of cool air coming from the upstream control volume, mixed with hot reversed air from the compressor.

The question is whether this reversed mass flow is mixing fully with the control volume mass upstream, effectively meaning the mass in these tubes and the air filter box. The large temperature increase seen in the measured data could also come from the fact that the temperature sensor was mounted very close to the compressor inlet. If the reversed mass stays in front of the temperature sensor for a longer period of time a higher temperature would show. This is however hard to estimate since the temperature sensor used is also sensitive for flow size and not only time.

To study the surge temperature, simulations using the test rig Simulink model are conducted. Using measured data as input, where so appropriate, the air filter control volume temperature, the temperature of the mass going backward in the compressor as well as the measured data are all shown in figure 3.7. In the figure, the output of the Simulink model as well as the measured value for the compressor inlet temperature are seen. The grey signal in the background is the modeled compressor inlet temperature. The reason for the large oscillations in this temperature is that it describes both forward flow as well as reversed flow. The temperature of the forward flow is taken as the temperature of the control volume upstream the compressor. In the case of surge the air is taken from the downstream control volume. This air is already heated. In the Simulink model a perfect and instantaneous mixing of the flows is said to occur in all control volumes. Using this information it is assumed that the mass flow does not fully mix with the mass of the control volume. In figure 3.7 an efficiency of 0.2 for negative mass flow is used. This simple approach gives a satisfactory behavior.

Shaft speed variations during surge

Once a value for the compressor efficiency for reversed mass flow has been determined, the shaft speed variations can be investigated. When investigating the shaft speed variations or using another term differences in produced and consumed torque, different data must be used. If a constant shaft speed test equipment is used, the compressor torque has to be measured or estimated. If a variable shaft speed measurement is used the shaft speed has to be accurately measured and/or the driving torque has to be estimated. The test rig data does not contain any information about applied/produced torque but the data collected in the engine test cell contains information about the shaft speed variations at least.

In this section the variations in shaft speed from figure 3.2 are to be modeled. To be able to study these variations the developed MVEM model is used. The model is run in operating points close to these given in the data, for one of the two available surge periods. The most important values of the
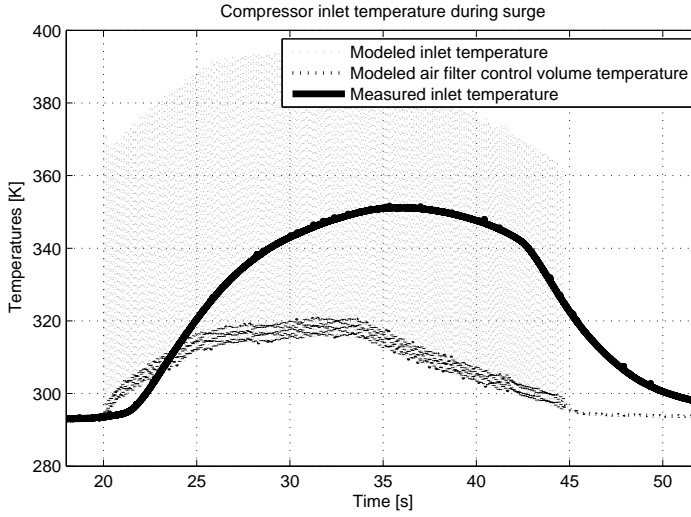
Figure 3.7: Figure shows modeled upstream control volume and compressor inlet temperature and measured inlet temperature.

chosen operating point were

$$
\begin{cases}
\Pi_c & = 1.85\,[-] \\
N_{tc} & = 120.000\,[rpm] \\
W_{af} & = 0.054\,[kg/s] \\
T_{af} & = 313\,[K]
\end{cases}
$$

When the Simulink model has stabilized in this operating point a surge cycle is induced by closing the throttle. The model and the measured data shows good agreement. The bandwidth of the shaft speed sensor used is not high enough to fully detect the quick changes in shaft speed. The general descending trend in shaft speed, in the measured data, is broken off during the surge cycles and for some of them a small increase in speed can be seen. The data also shows a time delay of about 5 [ms] due to the sensor and measurement equipment. The results are shown in figure 3.8. The initial operating point of the model has a higher N_{tc}. This is due to difficulties attaining the exact operating point. The model also shows a slower descending shaft speed when closing the throttle. This could be due to a bad compressor friction model.

To study the effect of a larger compressor friction term simulations were conducted using the developed MVEM Simulink model. To get the same relative decrease in shaft speed the friction term had to be raised to a value 15-20 times higher than used in the original model. Greater friction during surge could be due to the turbocharger shaking heavily during surge. This

means that the force acting on the shaft is greatly increased. A larger (normal) force, assuming the same friction coefficient, means that the frictional force increases.

Parameter estimation and sensitivity

The temperature of the air going upstream during a surge cycle is mainly a function of the compressor efficiency for reversed mass flows, but also of the downstream efficiency since this gives the temperature in the downstream control volume. The effect on the shaft speed variations during surge is small for different compressor efficiencies. A higher shaft friction can be used to smooth out the sharp shaft speed variations during surge shown, for example, in figure 3.8.
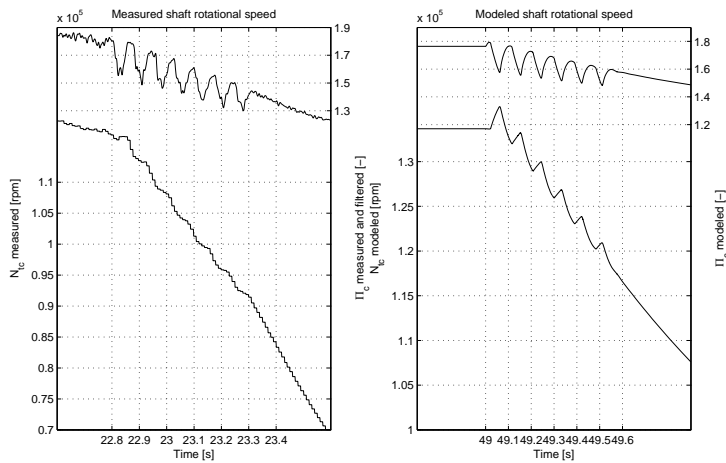

Figure 3.8: Left: Measured shaft speed variations during a surge period. Right: Modeled shaft speed showing surge induced from a operating point close to measured data. In both plots the pressure ratio is also shown as a reference.

3.3.3   Surge cycle starting point - surge line

The border line between the stable right side and the unstable left side of a compressor map is often referred to as the surge line. For operating points left of this line the compressor flow lines are said to be unstable and break down. The surge line is therefore of great interest when designing a compressor system or constructing a control system for a compressor. The surge point is very close to the peak or at the peak of each speed line [8, 9, 11].

The first question is if such a line exists? To study this the developed MVEM Simulink model is used. The shaft speed is locked during the simulation as is the engine speed. Wastegate position is kept constant and the surge valve is kept closed. Three different throttle closing slopes are used. The behavior is given in figure 3.9. It is clear that a definition is needed for when surge is said to start. To see when the mass flow of the compressor model changes sign the mass flow equation (2.6)

$$\frac{dW_c}{dt} = \frac{\pi D_c^2}{4L_c}(\hat{p}_c - p_c)$$

has to be investigated. This states that the modeled mass flow is the time integral of the difference between compressor pressure build up and the pressure in the control volume after the compressor.

When the downstream pressure exceeds the pressure build up, $p_c > \hat{p}_c$, W_c decreases. This is valid for all throttle closings in figure 3.9 and in fact for every possible W_c decrease. Because of this a surge line can not be defined as a point where the compressor pressure build up $\hat{p}_c$ differs from the downstream control volume pressure p_c. One way to define the surge starting point is when $\hat{p}_c$ starts to differ significantly from p_c. This is valid for all plots in figure 3.9. The figure shows that this in fact happens around the peak of the speed line. The simple surge line approximation is thus a good way to describe a surge line. The real surge starting point can however be anywhere in the compressor map. As soon as the operating point follows a path along which the pressure build up is ascending more slowly than the pressure downstream the compressor, the mass flow will continue to decrease. This implies that surge instability is highly dependent not just on the compressor characteristic but also the intercooler/throttle characteristic and the geometry in between compressor and throttle.

Further on $\hat{p}_c$ is dependent on both upstream temperature, T_{af}, as well as pressure, p_{af}, through the SAE-corrections. To study the effect of these factors surge is produced in the Simulink model and both corrected simulated variables and not corrected are shown in figure 3.10. The figure shows that the corrected mass flow is higher than the not corrected. For the shaft speed the opposite is true. Looking at one of the maps presented in section 2.2.3 both the N_{tc}-correction and the W_c-correction shifts $\hat{p}_c$ downwards. To stabilize a throttle closing a big $\hat{p}_c$ is desired since this is the only way to slow down a decrease in mass flow. This means keeping $N_{tc,corr}$ high and $W_{c,corr}$ close to the peak of the current speed line where the highest $\hat{p}_c$ is found for every speed line. Equation (2.1) shows that this would mean keeping p_{af} large and T_{af} small.

Most of the compressor maps available for this thesis have operating points left of the peak of each speed line. In the SAE standard for measuring automotive turbochargers it is stated that the speed lines making up the compressor map go from choke to surge. The standard defines the surge line, "Surge is the boundary of an area of severe flow reversal combined with

audible coughing and banging" [12]. The definition does not have a specific line. It is up to the persons, making the measurement, to stop measuring when they think "...audible coughing and banging" starts. This could be one of the causes for compressor maps having operating points that conflict with the approximated surge line.

Parameter estimation and sensitivity

None of the studied parameter variations have a major effect on the surge cycle starting point. As discussed in the previous section, it is more a question of where to define the starting point. Most of the model parameters affect how long time it takes before the first surge cycle is started. This is however more dependent on how fast the system is able to move around in the compressor map. The parameters having the greatest effect on this are the compressor control volume size and the compressor duct length.

3.4   Dynamic performance summary

In this chapter the phenomenon surge has been described. Different surge properties and surge data used was presented. The model parameters affecting different the surge properties were discussed and surge validation was also presented.

The compressor model developed is capable of producing and representing all the surge properties described in 3.2.1. It is easy to imitate one or two surge cycle properties and to get the good agreement between these, see figure 3.5. It is, however, hard to parameterize the model to have good agreement with all surge properties for all possible cases. On the other hand, a constant parameter approach already shows a correct behavior for all the surge properties, at least as long as exact numerical values for all surge variables are not required.

The lack of data in the surge region makes it hard to develop general methods for estimating the parameters of the compressor model when it comes to the surge region. Some of the model parameters need to be parameterized, e.g. in N_{tc}, to give a better agreement for more operating points.

Some manual tuning of the model parameters is required. Different model properties affect different surge properties. The surge pressure dip is most dependent on the compressor length L_c. It also shows a small dependence on the compressor characteristic for negative mass flow. The surge cycle time T_{cycle} shows a high dependency on control volume size. It is also highly dependent on the design parameter L_c. As with the pressure dip, T_{cycle} shows a small dependency on the compressor characteristic for negative mass flow. The temperature of the air going upstream during a surge cycle is primarily a function of the compressor efficiency during surge. The sharp edges of the modeled shaft speed variations can be smoothed out by increasing the
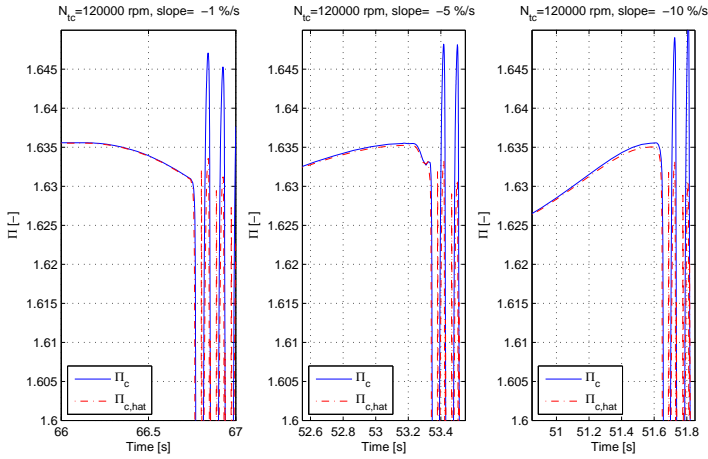
Figure 3.9: Π_c and $\hat{\Pi}_c$ for different throttle closing speeds. The pressures almost coincide before the surge period. Once the surge period has started the lines differ and it is this that causes the fast changes in mass flow. Left: Throttle closing speed $\frac{dA_{th}}{dt} = \frac{-1\%}{s}$, mid: $\frac{dA_{th}}{dt} = \frac{-5\%}{s}$, right: $\frac{dA_{th}}{dt} = \frac{-10\%}{s}$. The initial throttle area was 20% of $A_{th,max}$. The start of the throttle closing was $T = 50\ [s]$. The pressure where the surge cycles can be said to start is equal, independent of how fast the throttle is closed.
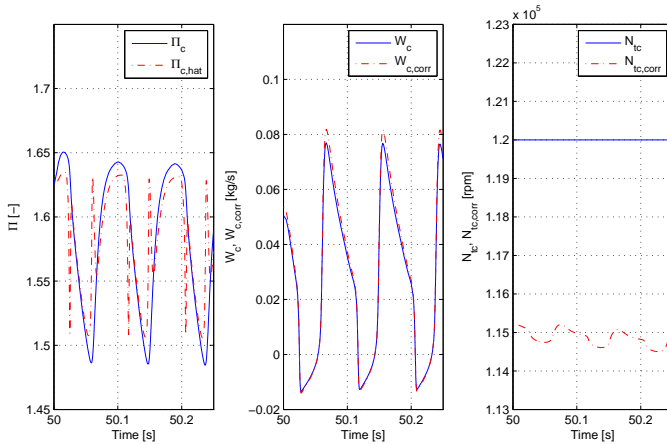

Figure 3.10: Left: Π_c and $\hat{\Pi}_c$. Mid and right: Simulated corrected and not corrected mass flow and shaft speed. $N_{tc,corr} < N_{tc}$ which gives a lower $\hat{p}_c$ value. $W_{c,corr} > W_c$ which also gives a (even) lower $\hat{p}_c$ value. A lower $\hat{p}_c$ decreases the time derivative of the compressor mass flow. This means that if the mass flow was descending prior to the change in $\hat{p}_c$ this descending will accelerate. If the mass flow was increasing the increase will slow down. The variation in shaft speed in the right plot is due to the temperature difference in the upstream control volume.

$Tq_{friction}$-term. The variations show a small dependency on η_c during flow reversal. None of the studied parameter variations have a major effect on the surge cycle starting point. The compressor characteristic for negative mass flow has great impact on the mass flow amplitudes of a surge cycle.

The question is also raised as to how good the standard [12] for measuring compressor maps is.

Chapter 4

Surge control and performance variables

This chapter describes different control strategies as well as how the controllers are implemented in Simulink. Methods to determine performance variables are described and evaluated. Available actuators for the controllers are modeled and described. Time delays and dynamics in the actuators are discussed as well.

4.1 The control problem

A control strategy is needed to avoid the unstable region of the compressor map. There have been many different approaches with a wide range of controllers investigated in the literature. Everything from avoidance controllers to active controllers that stabilize the compressor in the normal unstable region [3, 8] have been suggested. Some problems that have to be taken into consideration when designing controllers are time delays in sensors and actuators, mechanical delays and dynamics in actuators and sensors. The signal to the surge valve in today cars is binary so the surge valve is either ordered opened or closed. Continuous signals from the control systems have to be remodeled in the simulations in order to get more realistic simulations.

4.1.1 Control ideas

Knowledge about where surge occurs and when the compressor is about to enter surge is necessary when control methods are designed and validated. A approximated surge line is a good starting point when surge control is investigated. There are three main ideas in surge control and they are described below. The first is based on surge avoidance, the second on detection and avoidance and the last on stabilizing the compressor in the normal unstable

41

region [3, 8]. The first two control ideas have a performance variable to calculate the distance to the surge line. These variables will be investigated later in section 4.3. While the last control method stabilizes the compressor in the normal unstable region and is based on more complicated control methods.

Surge avoidance and protection

This strategy is based on keeping the compressor operating point at the right side of the surge line and away from regions close to the surge line. These regions are considered forbidden areas for the compressor. One way to limit the compressor operating region is to have a margin between the surge line and a so called surge avoidance line [3, 8]. This avoidance line sets new restrictions for the compressor. The surge margin depends on many things, how well known the surge line is, disturbances in the system and sensors and actuators. Since high pressure ratio and efficiency often lies close to the surge line, the performance of the compressor is reduced with this approach.

Surge detection and avoidance

This approach is based on that the control system starts to act if the compressor is about to enter surge or if surge is detected. This method is better than the above because the drawbacks with a surge margin are avoided during normal operating conditions. The drawbacks are that the control system needs fast actuators because when surge is detected the system needs to act fast. Surge has to be detected in an early stage so the control system has time to act [3, 8]. In an implementation phase the need of fast sensors and actuators can lead to problems because fast sensors and actuators are expensive or may be impossible to find.

Active surge control

Active surge control works in a totally different way compared to the methods mentioned above. This method stabilizes the compressor in the region where the compressor otherwise is in surge. The controller must have the possibility to reject disturbances, else the compressor can enter surge even if it has been stabilized in the normal unstable region of the compressor map. Methods for this active control approach can be linearization, bifurcation and lyapunov functions, see [8] for more information about active controllers.

4.2   Available actuators

To implement a surge avoiding controller there is a need for actuators. These affect the compressor operating point in the map. Actuators studied in this thesis are the surge valve and the waste gate. The effect they have on the

compressor operating point and how they can be modeled in Simulink are presented in this section.

4.2.1 Surge valve

The surge valve is also referred to as bypass valve or recycling valve. The purpose with this valve is to quickly recycle the compressed air from the volume after the compressor, so that the pressure after the compressor decreases. This is needed due to the slow dynamics in shaft speed. It is not possible to decrease the shaft speed fast enough when the compressor is about to enter surge. Opening the surge valve decrease the pressure ratio over the compressor by leading a part of the mass flow that comes from the compressor back to before the compressor and mixes this air with the air from the air filter.

The surge valve is modeled in Simulink with already available blocks from MVEM library. One adiabatic mixer for mixing gases from the air filter and the gas going back through the surge valve. A compressible restriction to model the surge valve and its opening. When the specific heat constant, c_p, is the same for the air upstream and downstream from the compressor, the adiabatic mixer is modeled as follows, see [6]

$$T_{mix} = \frac{W_{sv}T_c + W_{af}T_{af}}{W_{sv} + W_{af}}$$
$$W_{tot} = W_{sv} + W_{af} \tag{4.1}$$

The equation for the compressible restriction [6] is

$$W_{sv} = \frac{A_{eff}p_c}{\sqrt{RT_c}}\Psi\left(\Pi_{sv}\right) \tag{4.2}$$

The flow characteristic is represented by $\Psi\left(\Pi_{sv}\right)$

$$\Psi\left(\Pi_{sv}\right) = \begin{cases} \sqrt{\frac{2\gamma}{\gamma-1}\left(\Pi_{sv}^{\frac{2}{\gamma}} - \Pi_{sv}^{\frac{\gamma+1}{\gamma}}\right)} & for\ \Pi_{sv} > \Pi_{sv,crit} \\[3ex] \sqrt{\frac{2\gamma}{\gamma-1}\left(\Pi_{sv,crit}^{\frac{2}{\gamma-1}} - \Pi_{sv,crit}^{\frac{\gamma+1}{\gamma-1}}\right)} & otherwise \end{cases}$$
$$\Pi_{sv} = \frac{p_{af}}{p_c},\ \Pi_{sv,crit} = \left(\frac{2}{\gamma+1}\right)^{\frac{\gamma}{\gamma-1}} \tag{4.3}$$

Equation (4.2) gives how much mass flow the surge valve can recycle depending on effective valve area, temperature after the compressor and the pressure ratio over the valve. The pressure ratio over the surge valve is the inverted pressure ratio over the compressor. Equation (4.2) leads to a design parameter in terms of valve area, for the amount of mass flow the surge valve can recycle.

A maximum effective area of $1.14 \cdot 10^{-4}\,[m^2]$ is suggested in [15]. Under
the conditions that the temperature after the compressor is constant and that
there is no flow through the throttle, the suggested area can only recycle a
mass flow of $0.047\,[kg/s]$ at pressure ratio 1.7 and still keep the compressor
from surge for the compressor map shown in figure 4.1. At higher pressure
ratios the valve is unable to recycle the amount of mass flow needed to keep
the compressor in the stable region. If the compressors maximum shaft speed
and the pressure that the compressor is allowed to build is known, then the
area for the surge valve can be designed so it can recycle enough mass flow
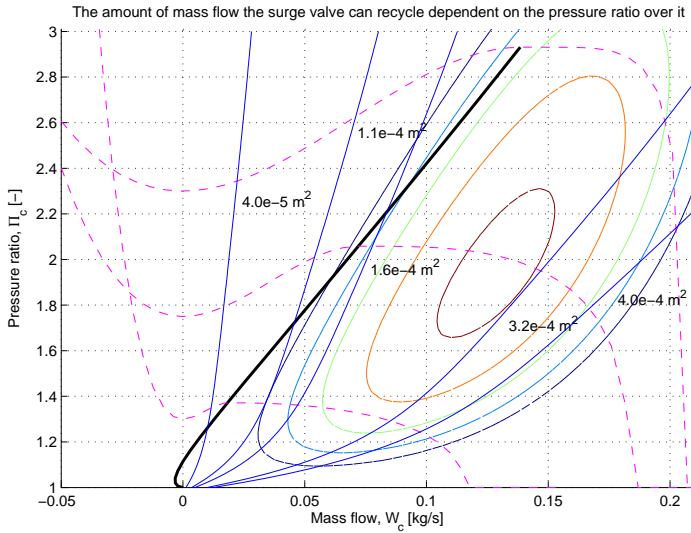for the worst case scenario of $W_{th} = 0$.

Figure 4.1: Shown here is a compressor map with different lines that represent
different surge valve areas. It shows how much mass flow the surge valve
can recycle depending on pressure ratio over the compressor and surge valve
effective area.

4.2.2   Waste gate

A turbocharged engine only runs with closed waste gate at very low engine
speeds. The waste gate is one important actuator available for controlling the
compressors performance and the operating point. The waste gate position
affects the torque that the turbine side gives to the compressor side and ac-
cordingly affects the shaft speed and the mass flow on the compressor side.
Figure 4.2 shows how the compressor operating point moves in the compres-
sor map for fixed waste gate positions. The throttle is fixed at 30% open and

the engine speed goes from 1500 $[rpm]$ to 4000 $[rpm]$. The operating point moves further down to the right the more open the waste gate is. The pressure ratio decreases for the same mass flow with an increase in waste gate opening. The waste gate is important for limiting the shaft speed and compressor pressure. When the engine operates under normal conditions the waste gate is important for avoiding surge. If the waste gate is kept closed the compressor can be forced into surge for higher engine speeds.
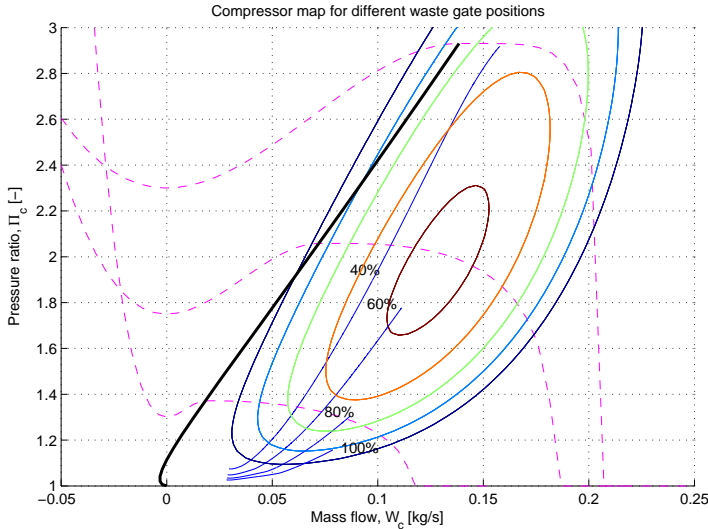

Figure 4.2: Shows how different waste gate positions affect the compressor operating point in a compressor map. The throttle is fixed and the engine speed goes from 1500 to 4000 $[rpm]$ with different waste gate positions.

4.3   Distances to surge

Different methods for determining a distance to the surge line are mentioned and discussed here. They are all implemented and tested in Simulink. Most of the them are based on different types of margins to the surge line. Since the surge line is an approximation of where surge is likely to occur there will be problems when deciding on how close to the surge line the compressor is allowed to work. A larger margin gives more safety to the system but with the drawback that the performance might decrease.

4.3.1   Distance in mass flow direction

If a surge line is given in a compressor map, a simple and used method is to take the mass flow to the surge line as a distance to surge. A margin can then be decided upon if there is uncertainty where the compressor enters surge. The response time in sensors and possibilities for disturbances in the system also affects the margins size. This has been been proposed in [4] among others.

Figure 4.3 shows a compressor map with a control line and an approximated surge line. The thick solid line is the surge line and the thin solid line is the control line. The area between these two lines is referred to as the surge margin. This is later referred to as ΔW_{ref} for the controllers.
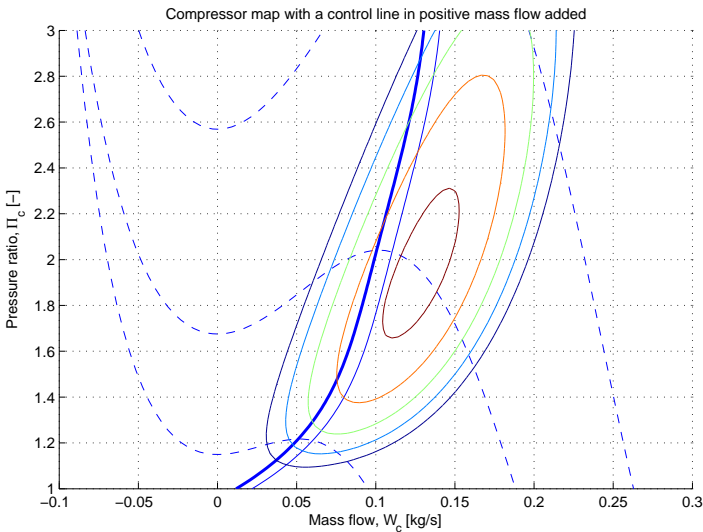

Figure 4.3: Compressor map with a surge line and a control line added in positive mass flow direction. The control line lies $0.01\ [kg/s]$ from the surge line. The thicker solid line is the surge line and the less thick solid line is the control line.

A distance in mass flow direction is a very simple method and this method is of great value in an implementation phase. It is also helpful when discussing controllers using ΔW_{ref} as performance variable. But also it has some drawbacks, limiting the stable operating region of the compressor since the control system starts to act when the compressor crosses the control line and a negative throttle demand is detected. A consequence is that the highest pressure for a specific speed line never can be reached when the throttle is closed. This is because the highest pressure is at the surge line and the

controller avoids this point in the compressor map.

4.3.2 Distance as the length of a normal vector to surge line

Another possible method is a modified version of the one given in 4.3.1. The main principle is to decide a distance in the direction of the normal vector of the surge line, the length of the normal vector depends on sensor response time and disturbances. It has the same drawback as a control line using ΔW_{ref}, the operating region for the compressor is limited. The control system starts to act as soon as the distance to the surge line is small enough. It is a different distance compared to the one given in 4.3.1 and it is harder to see the distance by directly looking at a compressor map.

4.3.3 Time to surge distance

This section discusses different approaches to determine the time it takes for the compressor to enter surge from every point in the compressor map. The compressor surge line is known and also that a fast negative change in throttle position makes the compressor go into surge. Assuming that the operating point follows a speed line into surge, makes this method possible to investigate.

Basic assumptions

Between the compressor and the throttle there are pipes and an intercooler. The pipes are modeled as control volumes in Simulink. These volumes and the intercooler restriction are modeled like one single volume when a time to surge is to be calculated using this method. The modeled volume is assumed to work as an isothermal model which is an important part of this calculation. The isothermal equation is the same as for a control volumes in MVEM_lib, see [6]. Looks like equation (4.4), under the assumptions that the throttle is closed and no mass flow passes through it. The isothermal equation has to be used to solve the time it takes for the compressor to enter surge.

$$\begin{cases} \frac{dp}{dt} = \frac{RT}{V} W_c(p(t), N_{tc}) \\ p(0) = p_{init} \end{cases} \qquad (4.4)$$

p_{init} is the initial pressure in the modeled volume, under the assumption that the pressure after the air filter is constant. T is the temperature in the modeled volume and it is set to a constant temperature. V is the merged volume of the pipes and the intercooler between the compressor and the throttle. R is the air constant in the modeled volume. The time for the compressor to reach the

surge line is now calculated with a rearrangement of equation (4.4) to

$$
\begin{cases}
\frac{dp}{dt} = \frac{RT}{V} W_c(p(t), N_{tc}) \\
p_{surge} - p_{init} = \frac{RT}{V} \int\limits_{0}^{t_{surge}} W(p(t), N_{tc}) dt \\
p(0) = p_{init}
\end{cases}
\tag{4.5}
$$

The parameters with subscript *surge* indicates the mass flow or pressure on the surge line for the speed line the compressor operating point are following on the way into surge. The subscript *init* stands for the operating point the compressor is at initially. The easiest way to approximate $W = W(p(t), N_{tc})$ is to use a triangle with edges in (W_{surge}, Π_{surge}) to the upper left, (W_{init}, Π_{init}) to the lower right and the third edge at (W_{surge}, Π_{init}). In figure 4.4 the triangle is shown.
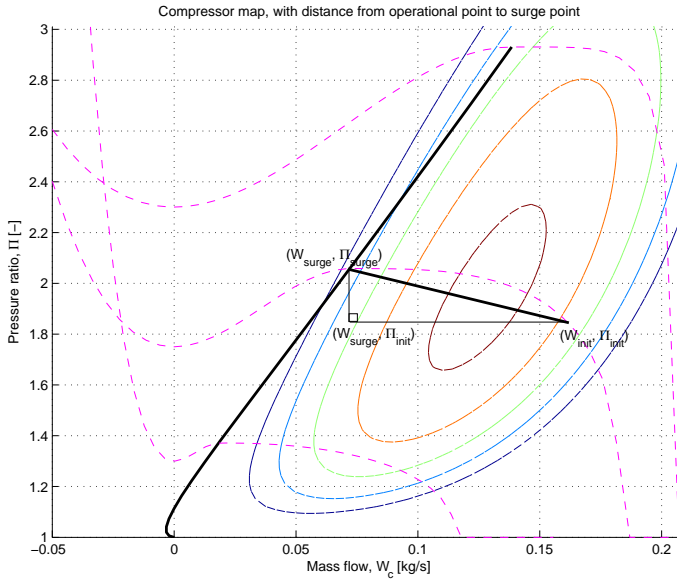

Figure 4.4: Compressor map that shows the path from the initial operating point to the surge point, when a shortest time to surge is calculated with the help of an isothermal model.

t_{surge} will give a time to surge for the shortest distance to the surge line. This time is a minimum time to surge. It will be a better approximation the closer the compressor operating point is to the surge line, but a worse approximation far away from the surge line. From the compressor characteristic it follows that t_{surge} is smaller than the actual time the further away from the

surge line the point (W_{init}, Π_{init}) is. But the actual time and calculated time gets better agreement closer to the surge line. In figure 4.5 and 4.6 time to surge is shown for two different compressors and a clear individual behavior is noticed in the figures.

Different solving strategies and implementation issues

The first and the most obvious solution is to have t_{surge} as a function of the current pressure after the compressor. This works very well for simulations when the surge valve is closed. t_{surge} passes zero when the compressor crosses the surge line in the compressor map. With a control strategy based on the surge valve as actuator, this approach does not work as intended. This implemented t_{surge} never passes zero when the compressor passes the surge line if the surge valve is opened.

   An explanation for this behavior is that the differential equation is very sensitive around the surge line. Opening the surge valve would make the calculations more inaccurate than with a closed surge valve. This is because the pressure after the compressor suddenly drops when the surge valves opens and the equations (4.4) and (4.5) do not model this effect. This model is based on the compressor having a fixed shaft speed on the way into surge and this is not the case in reality. The speed is decreasing slowly when a negative change in throttle has been done. Thus the real pressure at the surge line is lower than what the model has assumed.

   A second and more successful method to use is the difference in mass flow between the surge point and the mass flow from the compressor. This method works as intended showing $t_{surge} = 0$ when the compressors operating point passes the surge line, both with and without an opened surge valve. Instead of taking the pressure at the surge line and the operating point when equation (4.5) is solved, the pressure at the two points is calculated from the mass flow and the shaft speed at these points. The differential equation then can be solved. t_{surge} can now be used as a performance variable when control algorithms later on are investigated. Figure 4.5 and 4.6 show how the time to surge depend on the compressor characteristic.

4.4   P-controllers

P-controllers are one option when methods for avoiding surge are investigated. In this section different P-controllers are described. The performance variable will either be ΔW_{ref} from section 4.3.1 or t_{surge} from section 4.3.3. With these variables the control error can be calculated. The available actuator for the control system is the surge valve. The controllers are only described in the ideal case with zero time delays, dynamics and with continuous signals. The effects of such time delays and dynamics are discussed later.
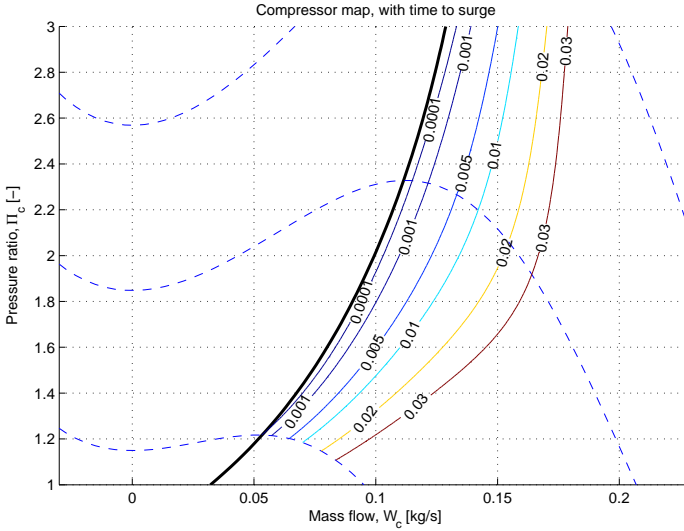
Figure 4.5: Compressor map that shows the time in seconds it takes for the compressor to enter surge if it follows a speed line on the way in to surge. Shown is a $\Psi(\Phi)$ compressor pressure build up model. The thicker line is the surge line for the compressor.
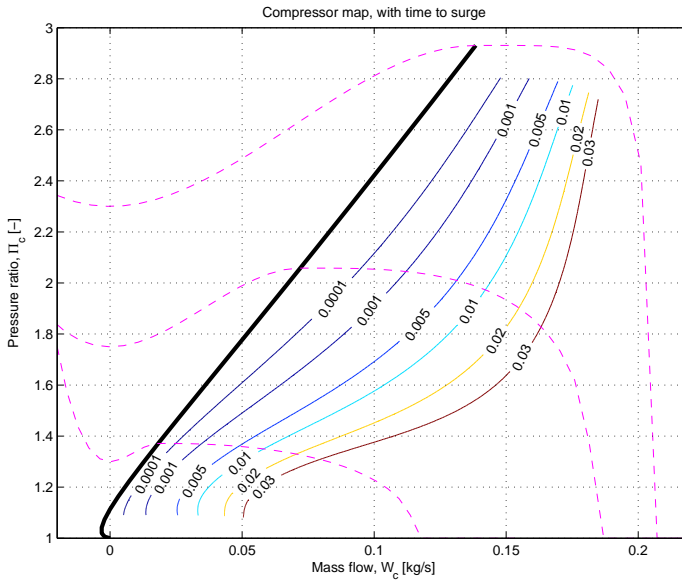

Figure 4.6: Compressor map that shows the time in seconds it takes for the compressor to enter surge if it follows a speed line on the way in to surge. Shown is an Ellipse compressor build up model. The thicker line is the surge line for the compressor.

The controllers are activated when a fast negative change in throttle position is noticed. They are deactivated with a positive change in throttle position. The throttle is used instead of demanded mass flow to the engine. This is because that signal is not available in the Simulink model. If the controllers are active all the time there are limitations in the pressure build up. Activating the controllers under short periods of time also lead to problems if a negative change in throttle is noticed very close to the surge line. The controllers are most likely unable to keep the compressor from surge if time delays and dynamics are introduced in the system.

4.4.1 P-controllers based on ΔW_{ref}

The mass flow controllers are based on the equation in section 4.3.1 to estimate the control error. The control error is calculated according to

$$e(t) = \Delta W_{ref} - (W_c - W_{surge}) \tag{4.6}$$

ΔW_{ref} is the reference mass flow from section 4.3.1. W_c is the compressor mass flow and W_{surge} is the mass flow at the surge line for a specific speed line. The value of ΔW_{ref} depends on different things like the actuator response time, noise in the system and the uncertainty of the surge line approximation. In the ideal case those factors are not a problem and ΔW_{ref} can go toward zero.

P-controller that opens the surge valve

A normal P-controller looks like equation (4.7) with the control error estimated according to equation (4.6). $u(t)$ is the control signal to the surge valve and is limited between zero and one. This controller starts to open the valve when the mass flow passes the reference mass flow.

$$u(t) = K_p e(t) \tag{4.7}$$

P-controller that closes the surge valve

A modified version of the controller above one is equation (4.8) with the control error (4.6). The difference compared to equation (4.7) is that this controller closes the valve the more negative $e(t)$ becomes. If ΔW_{ref} is passed it keeps the surge valve fully opened.

$$u(t) = 1 + K_p e(t) \tag{4.8}$$

4.4.2 P-controllers based on t_{surge}

The controllers presented here are very close connected to the ones that were based on ΔW_{ref}. The controllers are based on the performance variable

suggested in section 4.3.3, where the control error is calculated according
to equation (4.9). t_{ref} is the reference time and same as in the mass flow
description this value depends on things like response time in actuators and
uncertainty in the surge line. t_{surge} is the compressor's time to the surge line.
The division with t_{ref} is only a scale factor to give better error values.

$$e(t) = \frac{t_{ref} - t_{surge}}{t_{ref}} \qquad (4.9)$$

This controller will use equation (4.7) with the error (4.9) if it is wanted that
the surge valve shall open after t_{surge} has passed t_{ref}. If the controller shall
close the surge valve the further away from the reference the compressor op-
erating point, is equation (4.8) an option.

4.5   Open loop system and forward control

In the following two different controllers based on forward control and open
loop systems are presented. The first uses the knowledge about the surge
valve and the throttle characteristics. The second is based on a pressure dif-
ference that opens the surge valve and is similar to what is used in production
cars of today.

4.5.1   Open loop mass flow controller, W_{sv}-controller

This controller combines the knowledge about the surge valve discussed in
section 4.2.1 and the knowledge about how long time it takes for the com-
pressor to enter surge when a negative step in throttle is noticed, section 4.3.3.
From the surge line in a compressor map it is known where the compressor
enters surge. This gives how much mass flow between the surge line and zero
mass flow there is, given a shaft speed. The throttle is modeled the same way
as the surge valve, using a compressible restriction, equation (4.2) from the
MVEM library. This gives how much mass flow that passes through the throt-
tle into the engine. The difference between the surge mass flow and the mass
flow passing the throttle, gives the amount of mass flow the surge valve shall
recycle to avoid surge. The surge valve is then opened so the right amount of
mass flow passes through it. This is seen in equation (4.10). W_{sv} is the mass
flow the surge valve needs to recycle, W_{surge} is the mass flow at the surge
line and W_{th} is the mass flow through the throttle.

$$W_{sv} = W_{surge} - W_{th} \qquad (4.10)$$

The signal to the surge valve from the controller is given by equation (4.11).
When the surge valve shall open depends on the delays and dynamics in
the system. In the ideal case the valve can open near the surge line. The
opening of the surge valve is delayed with $\hat{u}(t - T) = u(t)$ where $T =$

$\max\left(\tau - t_{surge}, 0\right)$. τ is the sum of the time delays and the dynamics time constants in the surge valve and t_{surge} is time to surge given from section 4.3.3.

$$u(t) = \min\left(\frac{A_{needed}}{A_{eff}}, 1\right)$$
$$A_{needed} = \frac{W_{sv}\sqrt{RT_c}}{p_c \Psi\left(\Pi_{sv}\right)} \tag{4.11}$$

Where $\Psi\left(\Pi_{sv}\right)$ is given from equation (4.3).

4.5.2 Pressure difference open loop controller, $\triangle p$-controller

This is a modified version of systems currently used in production cars. The idea is to give a fail safe controller that avoids surge. The price is that the performance is limited more than necessary. The controller uses the pressure after the throttle, the intake manifold pressure, known as p_{im} and the ambient pressure, p_{amb}. The pressure difference is calculated as $\Delta p = p_{amb} - p_{im}$, from this pressure difference it is decided if the surge valve is to be opened or closed. The valve starts to open if the pressure difference is p_{low} and the valve is fully opened at a difference of p_{high}.

$$\begin{array}{lll} & \Delta p < p_{low} & \Rightarrow u(t) = 0 \\ p_{low} \leq & \Delta p < p_{high} & \Rightarrow u(t) = \frac{\Delta p}{p_{high}-p_{low}} - \frac{p_{low}}{p_{high}-p_{low}} \\ & \Delta p \geq p_{high} & \Rightarrow u(t) = 1 \end{array} \tag{4.12}$$

Where $0 < p_{low} < p_{high} \leq p_{amb}$.

4.6 Pulse Width Modulating, time delays and dynamics

When trying to make a more realistic case that represents the system in a production car, time delays for pressurizing the surge valve and the hose must be modeled in Simulink. The dynamics in the surge valve has to be modeled as well. The surge valve is not a continuous actuator, so Pulse Width Modulating (PWM) of the continuous signal from the control system gives the surge valve a binary signal. Figure 4.7 shows how these are implemented and modeled in Simulink. The signal goes through the PWM and then through a time delay followed by the dynamics for the surge valve.

4.6.1 Time delay and dynamics

Time delays and dynamics in the surge valve can easily be modeled in Simulink with the help of common blocks. The time delay is modeled with the help of a transport delay. The dynamics in the surge valve is modeled with the help
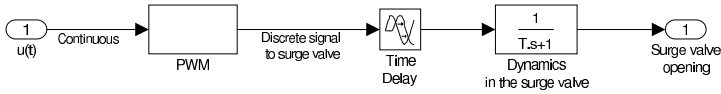
Figure 4.7: Pulse Width Modulated signal to the surge valve with time delay and dynamics, as implemented in Simulink.

of a first order transfer function. In [15] a time constant for the dynamics of 25 $[ms]$ and a time delay of 25 $[ms]$ is suggested. These numbers are adopted for the surge valve characteristics that will be used later when these are introduced in the Simulink model.

Time delay in the actuator

Time delays is a problem when the compressor is in regions with t_{surge} less than the time delay. The surge valve is not opened before the compressor has passed the surge line and thus enters surge. All suggested control approaches have this problem. Controllers that are based on t_{surge} has a straight forward method to tell if the controller is able to handle the delay or not, t_{surge} can always be compared to the time delays.

Dynamics in the actuator

The surge valve dynamics leads to the same problem as with a time delay. The difference is that here the valve will start to open but have not opened enough to recycle the requested amount of mass flow before the compressor enters surge. This effect can be slightly compensated for with a bigger surge valve area or with a larger K_p value in a feedback controller.

Figure 4.8 shows how the controller in section 4.4.2 acts with $t_{surge} < t_{ref}$ when a negative change in throttle area is done. The plot to the left has an effective surge valve area of $1.6 \cdot 10^{-4}$ $[m^2]$ and the right has an area of $2.4 \cdot 10^{-4}$ $[m^2]$. Assuming the same dynamics in the surge valve, the smaller surge valve area can not prevent the compressor from entering surge while the larger area can. In the ideal case both of the suggested areas should have been able to avoid surge according to section 4.2.1.

4.6.2   Pulse Width Modulation, PWM

The control signal to the surge valve is not a continuous signal in todays production car's, but a binary signal. Therefore the continuous control signal must go through a PWM in the Simulink implementation to study how the different suggested controllers can handle the more realistic situation. The Pulse Width Modulating takes the continuous signal from the control system
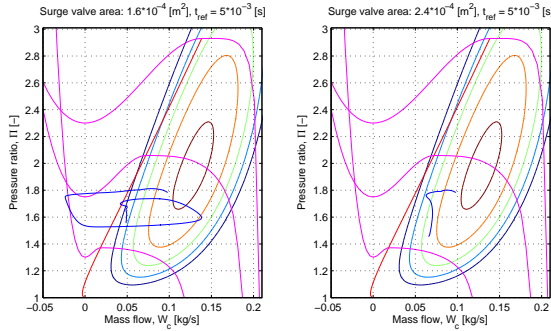
Figure 4.8: The left compressor map has a smaller surge valve area than the right. They both have the same surge valve dynamics. The right surge valve area setup is able to avoid surge while the left setup is not.

and gives the surge valve either zero or one. If the PWM gets a continuous signal of 0.3 the PWM sets 30% of the PWM period to one and the remaning 70% of the period to zero. The pulse frequency is choosen to $50\ [Hz]$, as is suggested in [15]. The PWM updates the continuous signal with $50\ [Hz]$ and decides how much of the PWM period the binary signal should be high. Compared to a continuous signal this leads to problems. If the last part of the PWM period is set to zero for a longer period of time, the compressor may enter surge. For example the PWM set the last 50%, $0.01\ [ms]$, of the period to zero and there is only $0.005\ [ms]$ to the surge line when the PWM changes from one to zero, the compressor enters surge.

4.7 Surge control and performance variables summary

There are many different approaches to handle the problem with surge. It can either be simple controllers like P-controllers and open loop controllers or more advanced controllers as described in section 4.1.1.

The most promising performance variable is a mass flow method described in section 4.3.1 or a time to surge method described in section 4.3.3. These variables are used by the P-controllers presented in section 4.4 for estimating the control error. Two open loop controllers are presented in section 4.5, where one is based on the amount of mass flow the surge valve can recycle and the other on a pressure difference.

The time to surge method in section 4.3.3, is based on an isothermal model, similar to the ones used for control volumes in MVEM_lib. In the control volume there are in and out flows, but this method considers the throt-

tle to be closed and zero mass flow through it, so there is only flow into the
volume. Further on, when designing this time measurement it is assumed
that compressor operating point follows a speed line into surge and that the
temperature in the control volume is constant.

The actuators for changing the compressor operating point in the map is
modeled in section 4.2. The purpose with a waste gate on the turbine side is
discussed and the effect the waste gate has on surge avoidance and limitations
in compressor mass flow is investigated. The more open the waste gate the
further down to the right the compressor operating point is moving in the
compressor map.

The surge valve and how the effective surge valve area affect the amount
of mass flow the surge valve can recycle is investigated in section 4.2. Under
the assumption that the temperature is constant, the surge valve is only able
to recycle a limited amount of mass flow depending on the effective area and
the pressure ratio over it. So the surge valve area can be be considered as a
design parameter, if it is known how much pressure the compressor is allowed
to build.

Time delays between the controller and the surge valve and dynamics in
the surge valve are introduced in section 4.6. The surge valve in production
cars is not able to handle continuous signals, so the signal from the imple-
mented controllers in Simulink have to be made binary with the help of Pulse
Width Modulating. This is described in section 4.6 as well.

Chapter 5

Control performance

This chapter presents how the different controllers suggested in chapter 4 handle a specific test case. Time delays, dynamics and Pulse Width Modulated control signals are introduced in the system to see the effect of these. The main signals used for performance comparison are the shaft speed and the engine net torque. These are natural measurements when evaluating the performance of the different controllers. The shaft speed is good because it shows how much pressure the compressor can build later on when the gear change is over. The higher speed, the more mass flow from the compressor and a faster pressure build up. The engine net torque is a good performance comparison variable since it shows how much the compressor performance affects the engine.

5.1   Test case

To quantify the performance a test cycle has to be determined. The most obvious way would be a case where the compressor can enter surge in some part of the test cycle since this is what the controllers shall avoid. A car in an acceleration phase, including a gear change, is therefore a good test case. The compressor enters surge easily due to a rapid negative change in throttle mass flow, i.e. when the throttle closes fast.

5.1.1   Quantified case

The test case is based on a car in an acceleration phase, for example when the car is accelerating from zero to hundred $[km/h]$. Since a full car model is not available in the simulations, this case is tested using the available engine model. In figure 5.1 an acceleration phase with fast gear changes is done in a real car. It shows a gear changes that are suppose to take about 0.5

seconds. The simulated test case can then be modeled as follows to give a good approximation of the measured acceleration.

The engine is run at $1000 \; [rpm]$ for one second with the throttle 10% open. The first second is to stabilize the mass flows and the pressures in the simulation. This is followed by an acceleration phase which is modeled as a ramp in engine speed up to $6000 \; [rpm]$ over four seconds. The next phase is a gear change of 0.5 seconds. During this period the engine speed is ramped down to $3000 \; [rpm]$. When the gear change is completed, the engine goes up to $6000 \; [rpm]$ in 4.5 seconds. The throttle is fully opened during the accelerations and during the gear change it is fully shut. The whole test case is ten seconds long where the time around the simulated gear change decides if the compressor will enter surge. Figure 5.2 shows throttle position and engine speed during the ten seconds of simulation.

This test cycle is an extreme case since there is no throttle dynamics. The throttle has dynamics in a real engine. This test can be seen as a worst case scenario for the controllers.

The drawback with tuning the controllers to this case is that they can be too aggressive in less extreme cases, so the engine performance is reduced for other situations. The pressure ratio over the compressor is reduced too much under a longer gear change so the controllers have no significant effect at the end of the gear change. Also that the performance differences of different controllers may be less obvious for a faster gear change where a higher pressure ratio and shaft speed may be maintained because the shaft speed have not been reduced enough. Because of these possible problems two other test cases are studied. One with a faster gear change taking 0.3 seconds and another with a gear change taking 2 seconds.

Limit shaft speed and pressure ratio

The compressor has in reality a limitation in speed because the possibility for the compressor to break down at high shaft speeds. Due to this a simple PID-controller is implemented in this test case engine model to control the maximum shaft speed and pressure after the compressor. The controller uses the waste gate as actuator and the pressure after the intercooler as performance variable. The reference pressure is set to $150 \; [Kpa]$.

A surge valve effective area of $1.6 \cdot 10^{-4} \; [m^2]$ is used. This effective area is able to recycle enough mass flow to keep the compressor from surge up to a pressure ratio around 2.2, in the ideal case, according to section 4.2.1.

5.2   Control performance of suggested controllers

With the test cases setup the controllers described in section 4.4 and 4.5 can be tested and evaluated. First it is done with no delays and with a continuous surge valve signal. After these simulations are done a PWM control signal,
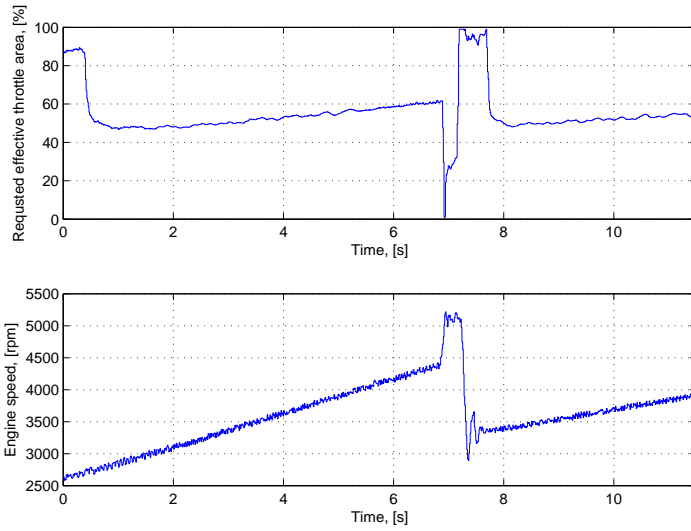
Figure 5.1: Throttle position and engine speed under an acceleration phase in a real car.
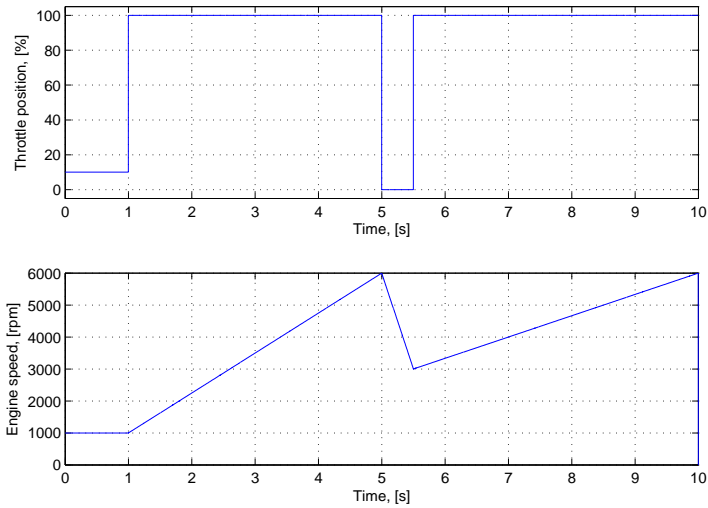

Figure 5.2: Throttle position and engine speed for the test case used in the simulations. The simulated gear change takes 0.5 seconds.

time delays, and dynamics are introduced in the system. Since P-controllers with ΔW_{ref} and t_{ref} as reference variables are very similar there are no discussions around mass flow controllers. t_{ref} is a more intuitive variable to use when time delays are introduced in the system.

5.2.1   Control systems with continuous control signal

The continuous case is studied to see if the controllers can avoid surge and if not, what modifications of the control parameters are needed so the controllers can avoid surge with a continuous control signal. Then time delays and dynamics are introduced and the effect of these are discussed.

P-controllers

There are no problems for the P-control systems to avoid surge. With both versions of the t_{surge} controller it is possible to let t_{ref} go toward zero and allow the compressor to operate closer to the surge line. The controllers are able to keep the compressor from surge with only a proportional part, but with the drawback that the control signal starts to oscillate more the smaller t_{ref} gets or the larger the K_p value gets. This behavior can be seen in figure 5.3, where $t_{ref} = 0.1 \, [ms]$ and different K_p values are used. Only the interesting part in the beginning of the controller's active period of the cycle is shown.
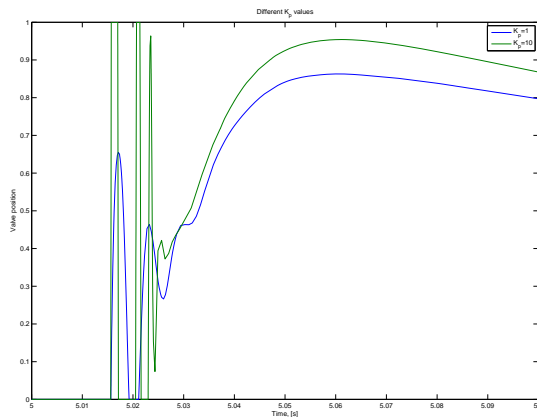

Figure 5.3: Different K_p values in a P-controller and the effect on the control signal from the different values. A larger K_p gives a more oscillative control signal.

Open loop mass flow controller, W_{sv}-controller

In the continuous case with no delays and A_{needed} for the surge valve it is impossible to avoid surge in most cases. A small modification of the equations in section 4.5.1 makes the controller avoid surge. Increasing A_{needed} with 50% directly gives an increase of the amount of mass flow the surge valve is able to recycle, according to equation (4.11). This gives a safety margin to the system when the suggested area to open is larger than the actual needed one. In figure 5.4 an increase in needed area is tested. The dashed line shows that the compressor has gone into surge without an increase in area while the solid line has a 50% increase in area and is therefore able to avoid surge.
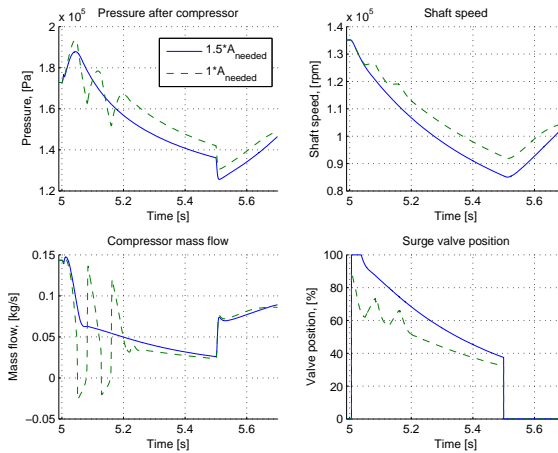

Figure 5.4: A 50% increase in A_{needed} keeps the compressor from surge for the W_{sv}-controller. The solid line shows a non surge behavior while the dashed has clearly gone into surge. The solid has the 50% larger surge valve area.

Comparison between continuous controllers without time constants

To see how the continuous controllers behave and to investigate which is the better one a couple simulation are needed. Those simulations are later reference cases when time delays, dynamics and a PWM are introduced in the system. The reference case has $t_{ref} = 15\ [ms]$ and $K_p = 1$ for the P-controllers. An increase in A_{needed} with 50% for the W_{sv}-controller is implemented. The P-controllers can be better tuned togheter with a I and D part, to get better performance but this can be very time consuming. Since the interesting part is to see if the controllers can handle time delays and dynamics in the surge valve a proportinal part is enough for this case.

In figure 5.5 the engine torque and compressor shaft speed is plotted for different ideal controllers and figure 5.6 shows the control signal to the surge valve. Seen in the figures is a 10.5% difference in shaft speed at time 5.5, between the W_{sv}-controller flow and the P-controller for closing the surge valve. At time 5.7 the difference is 6.1% in engine net torque and 6.8% in shaft speed. With a 0.5 second gear change the W_{sv}-controller is the most efficient keeping shaft speed and therefore geting a higher engine torque after the gear change. The worst controllers are the Δp-controller and the P-controllers that close the valve. These two are equally bad.
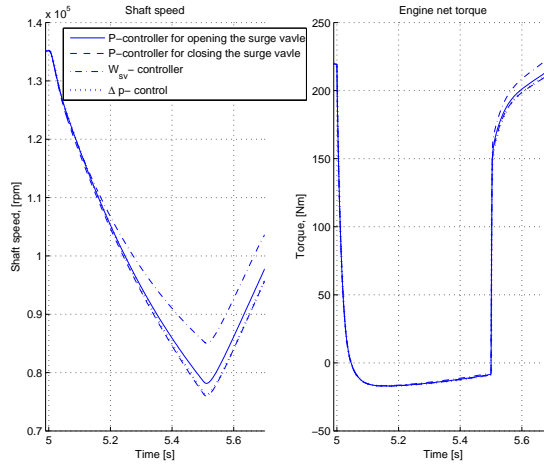

Figure 5.5: Engine torque and shaft speed for different controllers in the ideal case with a 0.5 second gear change. The W_{sv}-controller is clearly the better controller, seen in the higher shaft speed and higher engine net torque.

The same situation is studied for the 0.3 second gear change and this case shows a difference between the different controllers of 4.2% in shaft speed at time 5.3 and 0.6% at time 5.5. Engine torque has a 0.9% difference at time 5.5 shown in figure 5.7. This case, as with the 0.5 gear change, shows that the W_{sv}-controller keeps the highest shaft speed and engine torque during the gear change.

At the 2.0 seconds long gear change the difference at time 7 is 55.9% in shaft speed. At time 7.2 there is a 33.9% difference in shaft speed and 11.5% in engine torque. Figure 5.8 shows the engine torque and shaft speed for this simulation.

From these simulations some observations are done. The W_{sv}-controller is clearly the better controller, while the Δp-controller keeps the surge valve open during the whole gear change and is the worst together with the P-
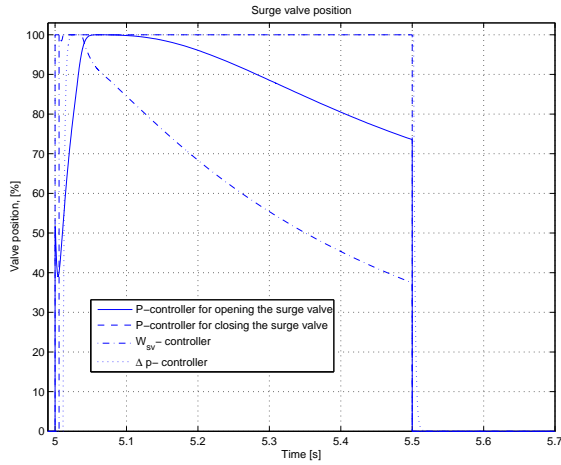
Figure 5.6: Control signal to the surge valve with different controllers, in the ideal case with a 0.5 second gear change.
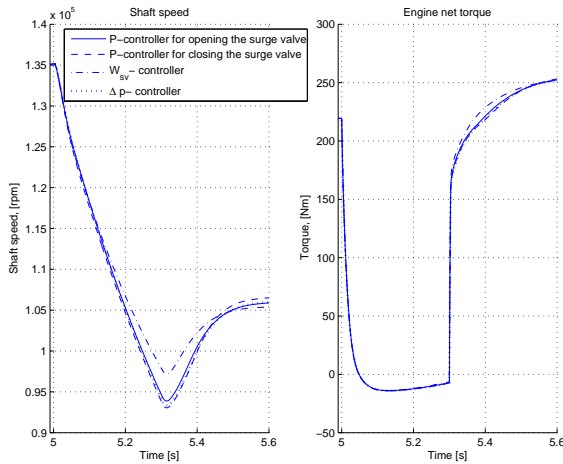

Figure 5.7: Engine torque and shaft speed with different controllers in the ideal case with a 0.3 second gear change. Here the difference between the controllers are smaller, but the W_{sv}-controller is still the best choice.

controller that closes the surge valve. One of the reasons why the P-controllers
are not better can be that t_{ref} in this case is set very high so that they can be
compared to simulations later when time delays and dynamics are introduced.
Figure 5.9 and 5.10 show the improvements made with a reference time of
0.1 $[ms]$ instead of 15 $[ms]$, with $K_p = 1$ for the P-controller that opens the
surge valve. The improvement is 5.2% in shaft speed and 6.1% in torque at
time 5.7. Another possible reason for the bad performance with the feedback
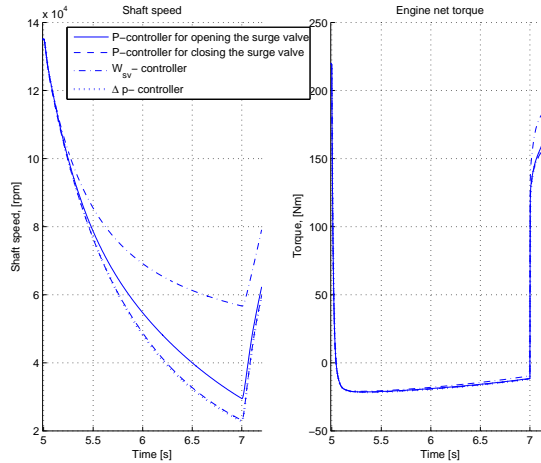controllers is badly tuned parameters.

Figure 5.8: Engine torque and shaft speed with different controllers, in the
ideal case with a 2.0 seconds gear change. Clearly the W_{sv}-controller is the
better one.

**Impact on control performance with time delays and dynamics in the
system**

The introduction of time delays in the continuous control signal to the surge
valve and dynamics in the surge valve lead to some problems when it comes
to control of the compressor. In section 4.6 are those problems described and
some common thoughts around the subject are given. This part focuses on
how the specific controllers behave and what problems there are when using
the test case.

   In [15] a time delay of 25 $[ms]$ is suggested and in the simulations is
t_{surge} much smaller when the gear change happens. Time delays longer than
t_{surge} at the gear change makes it impossible to avoid surge for all given
controllers except for the Δp-controller. With time delays the system can
handle, the performance is reduced with about 1% in engine torque and shaft

speed for the different controllers. This is a small decrease in performance compared to the difference between the controllers.

Dynamics in the surge valve when the control signal to the surge valve is continuous decreases the performance of the controllers. The effect is in the same range as with time delays. If the dynamics time constant is large the compressor will enter surge because the surge valve can not recycle mass flow fast enough. It is of great value to reduce the dynamics and the time delays as much as possible even if the surge valve is continuous, to obtain maximum performance.
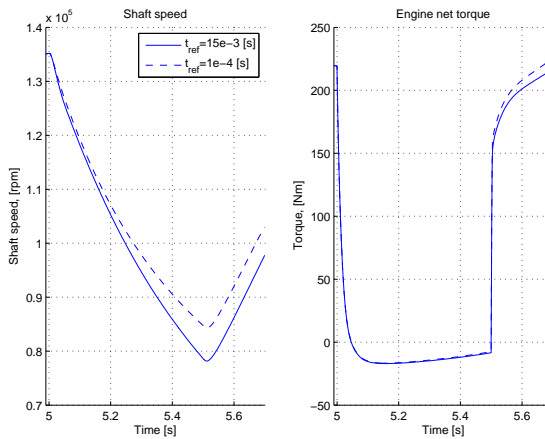

Figure 5.9: Engine torque and shaft speed with different t_{ref} for the P-controller and a 0.5 second gear change. A smaller t_{ref} increases the performance.

5.2.2 Pulse Width Modulated control signal

In section 4.6.2 it is described how the PWM is implemented and here the consequences of this implementation will be investigated closer. First is a PWM implemented without delays and dynamics, later are time delays and dynamics introduced. When a PWM is implemented and the continuous signal gives zero to the PWM at the gear change the surge valve is closed for the whole period of $20\,[ms]$. The compressor enters surge during this time if $u(t) = 0$ and if $t_{surge} < 20\,[ms]$ at the gear change.

Without dynamics or to fast dynamics there are problems in the end of the PWM period when the surge valve is closed. The compressor goes into surge if t_{surge} is less then the remaining time of the PWM period.
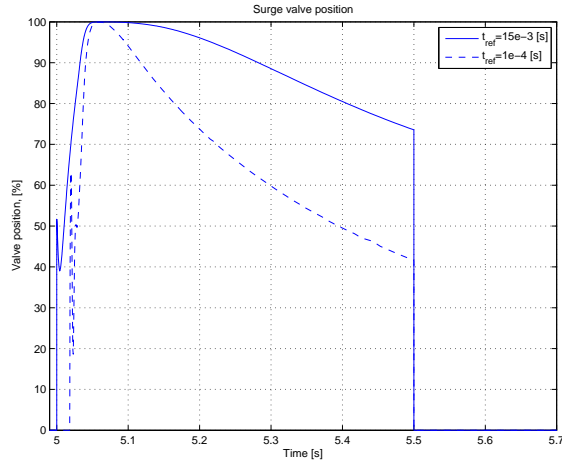
Figure 5.10: Control signal with different t_{ref} for a P-controller and a 0.5 second gear change.

Comparison of Pulse Width Modulated controllers

When the continuous signal is Pulse Width Modulated there are problems when there is no dynamics in the surge valve. Controllers that avoid surge with a continuous control signal can not avoid surge when the control signal is a PWM. The control signal starts to oscillate after a while when the PWM closes the surge valve in the end of the PWM periods. This leads to an oscillative mass flow and pressure. In the worst case the system can enter deep surge. Figure 5.11 shows the oscillations during a 0.5 second gear change.

The only controller able to avoid surge during all length of gear changes, among the suggested in section 4.4 and 4.5, is the Δp-controller. The PWM for this controller does not cause problems since the control signal demand fully opened surge valve during the whole gear change.

Impact on performance from time delays in the control system

A time delay between the binary signal from the PWM and the surge valve makes the compressor enter surge at the beginning of the gear change if the time delay is larger than t_{surge}. Figure 5.12 shows the shaft speed and the mass flow for a P-controller that opens the surge valve at the gear change. The dashed control signal in the figure is delayed with 25 [ms] while the solid is not. It shows that the compressor enters deep surge when the control signal is delayed before it starts to follow the oscillations that the PWM is causing. The compressor enters deep surge for a few surge cycles at the beginning
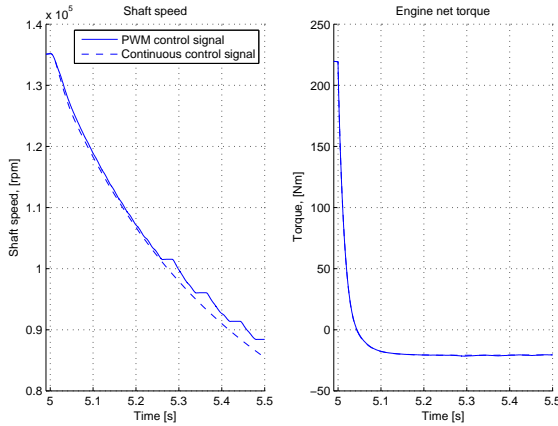
Figure 5.11: Pulse Width Modulated control signal that gives a surge like behavior after a while. when the PWM starts to oscillate. This is seen in the shaft speed where the solid line start to oscillate.

of the gear change. This is much more serious than the oscillations that the PWM itself is causing.

Impact on performance from dynamics in the surge valve

The effect of dynamics is also interesting to study and especially when the control signal to the surge valve is binary. A large time constant in the dynamics does not open the valve fast enough so the compressor goes in surge when a gear change is done. A smaller time constant in the dynamics makes the system more oscillative as mentioned above.

In figure 5.13 is the W_{sv}-controller shown during a 0.5 second gear change, with a time constant in the dynamics of $25\,[ms]$. This constant is large enough to avoid surge under this 0.5 second gear change shown in the figure. The decrease in shaft speed and engine net torque is 0.5% at time 5.7 compared to a continuous case. A smaller constant or a longer gear change would have made the compressor gone into the oscillations mentioned earlier.

The P-controllers can handle a smaller time constant in the dynamics under a short period of time. But larger constants is not possible because the compressor enters surge at the beginning of the gear change. In figure 5.14 it is shown that a large constant in the dynamics causes one surge cycle with the small increase in shaft speed at time 5.06. A time constant of $10\,[ms]$ in the dynamic can avoid surge but with a decrease in engine torque on 4.4% at time 5.7 compared to the continiuous control signal.
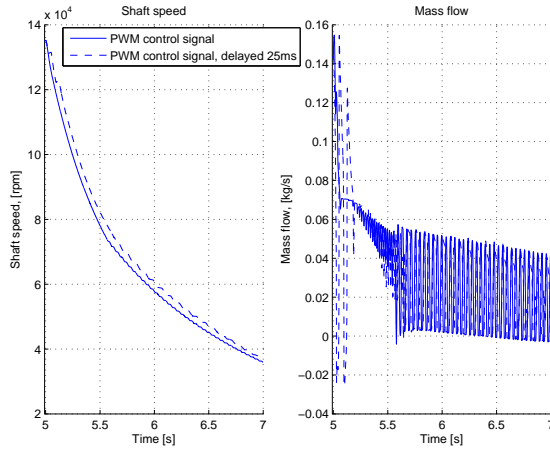
Figure 5.12: A time delayed Pulse Width Modulated control signal from a P-controller makes the compressor enter deep surge for a few cycles in the beginning of the gear change. The compressor then goes into a milder surge like behavior, like the non delayed PWM control signal.
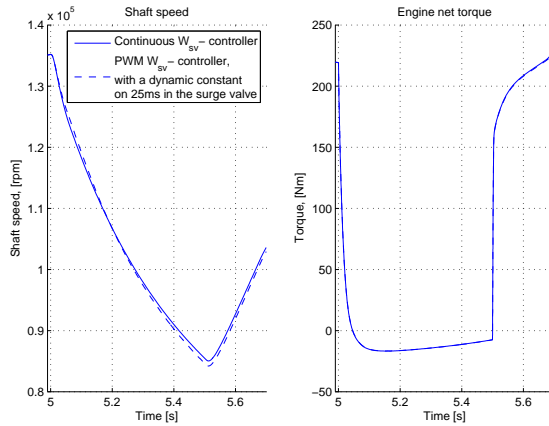

Figure 5.13: The figure shows a PWM W_{sv}-controller compared to the continuous case. A surge valve dynamics time constant of 25 $[ms]$ is used.
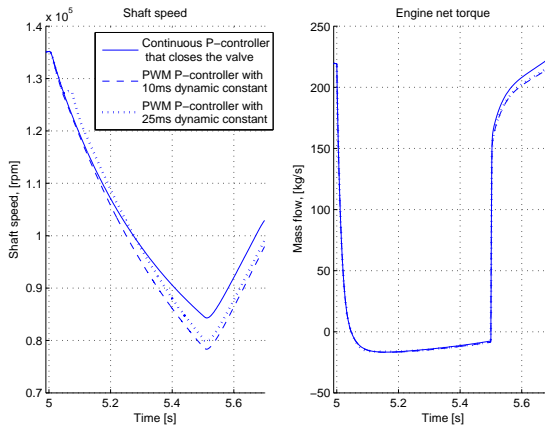
Figure 5.14: Different time constants in the surge valve dynamics, with a PWM control signal from a P-controller compared to the continuous case. The compressor enters surge with the large time constant, seen in the small increase in shaft speed at time $5.1\,[s]$.

5.3 Handling of time delays and dynamics

With the knowledge from the discussions above and from simulations it is noticed that effects of time delays, dynamics and the binary control signal limit the possibilities to control the compressor from surge.

Instead of the approach to activate the controllers when a negative throttle change is noticed, a better solution to use is the Δp-controller to open the surge valve. After the surge valve has opened, another controller tries to close the surge valve to get the compressor operating point as close to the surge line as possible. This because an increase in performance compared to keeping surge valve open during the whole gear change may be achieved. This approach gives a safety to the control system since the controllers closes the valve after it has been opened. The problem with time delays and dynamics in the system are also reduced. Instead of the controllers trying to just avoid surge, they also try to increase the performance. By closing the surge valve instead of having the surge valve open during the whole critical period when surge is avoided.

A similar solution was presented in section 4.4 but this controller opens the valve when a negative changes in throttle position is noticed, the problems with time delays and dynamics was still a problem. Now the opening is done with the help of the Δp-controller and this new control approach for closing the surge valve is active when $u(t) \neq 0$, seen in equation (4.12).

This method is tested in the same test cases as previous investigations with

a W_{sv}-controller and with a P-controller with $K_p = 1$ and $t_{ref} = 15\,[ms]$. A time delay of $25\,[ms]$ and a constant in the dynamics of $25\,[ms]$ are used.

Figure 5.15 shows how the controller decreases the performance compared to the reference cases in section 5.2.1. The problem with the compressor entering surge is avoided even with large time constants in the system. This was not possible with the previous approaches that used the throttle position to decide when the controllers should be active.
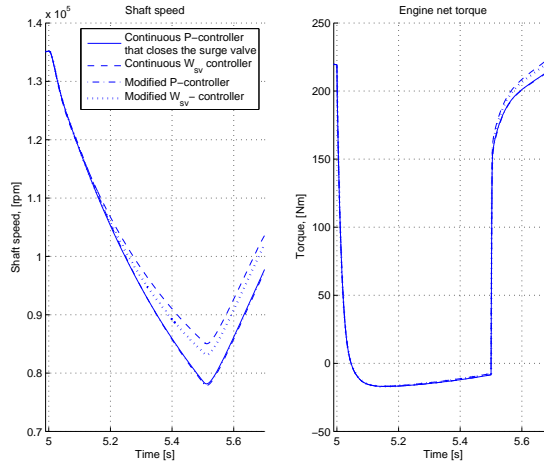

Figure 5.15: Reference continuous controller and a control approach that handles time constants are compared. Both a P-controller and a W_{sv}-controller have been compared. The latter controller is better.

The difference between the continuous P-controller and this new approach of P-controllers in the 0.5 second gear change is less then 0.5% in shaft speed and engine torque. For the W_{sv}-controllers the decrease is 1.2% in shaft speed and 1.9% in torque at time 5.7. These decreases are not so bad since these controllers have a Pulse Width Modulated signal with time delays and dynamics in the surge valve, compared to a continuous control signal.

This is an interesting approach since it is robust to delays and still has a good performance compared to the reference cases. In figure 5.15 it can also be seen that the W_{sv}-controller is clearly the better choice for maintaining shaft speed and also gives a higher engine torque in the beginning of the acceleration after the gear change.

5.4   Control performance summary

To see if the suggested controllers given in section 4.4 and 4.5 are good approaches to avoid surge a test case is developed. The test case is based on a gear change during an acceleration phase, see section 5.1.

With a continuous control signal, no time delays and dynamics in the system, the controllers avoid surge without any problems, seen in section 5.2.1. These simulations act as reference cases when the control signal is Pulse Width Modulated and when time delays and dynamics in the surge valve are introduced.

When a binary signal to the actuator is introduced, in section 5.2.2, the compressor often goes into surge. With time delays and dynamics introduced it is difficult for the investigated control structures to avoid surge, if the control signal to the surge valve is binary. Another approach, presented in section 5.3, similar to a P-controller that closes the surge valve is tested. This method works relatively well compared to the reference case, the decrease in performance is acceptable.

The conclusions of this chapter is that delays in the system makes surge control very complicated since there are only small time frames to act in. If it is possible to have a continuous surge valve the performance is the best achievable and the impact of time delays and dynamics in the system are not as serious as with a binary signal. The most critical part is when the surge valve shall open. Conditions leading to surge have to be detected very early so there is time for the surge valve to open before the compressor enters surge. As mentioned in section 5.3 there are ways to manage these problems.

The approach to close the surge valve, after it has been opened by a pressure difference instead of being opened by the controller, gives safety to the system. This approach reduces the problem with time delays, dynamics and PWM signals. The drawback is a small decrease in performance compared to the continuous case.

The best suggested controller both in the continuous case and otherwise is an open loop controller that controls the mass flow needed to be recycled through the surge valve.

Chapter 6

Future work

Different proposals for future investigations are given in this chapter.

- **Surge line:** Investigations of the stable operating points left of the surge line seen in the available compressor map data. The stabilized operating point to the left of the point of zero slope of the compressor characteristic (the approximated surge line) seen in most of the compressor maps available to this thesis would be interesting to investigate further.

- **Tuning of the P-controllers and introducing a full PID-controller:** The goal with this thesis was not to tune the best controller but to study the effect from time delays, dynamics in the actuators and PWM signals. It would thus be interesting to study the performance gains from a perfectly tuned PID-controller. Even the possible performance gains from more advanced controllers, e.g. MPC, would also be interesting to study.

Chapter 7

Summary and conclusions

Modeling and control of automotive turbo chargers are studied, using experimental data and simulation.

The sub models making up a surge capable compressor model are given in chapter 2. The equations presented are valid both for the normal operating region as well as the surge region of the compressor map. For the stationary region of the compressor map methods are found to automatically parameterize the compressor model. This is however harder for the surge region of the compressor map.

The developed compressor model is certainly capable of reproducing most of the surge properties described in section 3.2.1. There is not enough measured data available for developing scripts for parameterizing the surge region of the compressor model automatically. As seen in section 3.3 the surge representation of the model is capable of showing good agreement with measured data. When tuned for a specific surge property the model representation shows very good agreement. However, it is difficult to tune the model to handle all different surge properties simultaneously.

Some hand tuning of the model parameters is required to get the desired surge behavior. Different model properties affect different surge properties. The surge pressure dip is most dependent on the compressor length L_c. It also shows a small dependence on the compressor characteristic for negative mass flow. The surge cycle time T_{cycle} shows a high dependency on control volume size. It is also highly dependent on the design parameter L_c. As with the pressure dip, T_{cycle} shows a small dependency on the compressor characteristic for negative mass flow. The temperature of the air going upstream during a surge cycle is primarily a function of the compressor efficiency during surge. The sharp edges of the modeled shaft speed variations can be smoothed out by increasing the $Tq_{friction}$-term. The variations show a small dependency on η_c during flow reversal.

The compressor characteristic for negative mass flows has a great impact on the mass flow amplitudes of a surge cycle. The parameter sensitivity is

also studied more thoroughly in the subsections of section 3.3.

Surge avoidance poses a complicated control problem because of the small time frames. A method to determine the minimum, worst case, time to surge from different operating points is presented. This shows that it is only a matter of milliseconds, after a sharp negative change in throttle position, before the compressor enters surge. It is, therefore, a big challenge to get the desired control performance with time delays, dynamics and the fact that the surge valve only takes binary signals.

The two available actuators, that are investigated, are shown to be able to construct good controllers. The investigation of the surge valve gives a method for estimating the needed surge valve area. A controller that uses the information gained from the surge valve investigation is developed. The controller uses the surge line and the shaft speed to determine how much the surge valve should open.

It is hard to construct a robust control system that opens the surge valve due to the small time frames. Therefore, instead of opening the surge valve with the help of the control system, it is better to open the surge valve as soon as surge may occur. This method is similar to what today's control systems do. The opening can be done with the help of a pressure difference, e.g. the difference $p_{amb} - p_{im}$. The closing of the surge valve is thereafter controlled by the surge controller. The difference is that the here developed controllers try to keep the compressor operating point as close to the surge line as possible to maximize the performance whereas the currently used systems wastes too much pressure. The system can be made to handle uncertainties in time delays and various dynamics in the actuators and still increase the performance compared to the currently used production systems.

Among the suggested controllers, one approach shows a better performance compared to the other suggested controllers. This controller is based on the mass flow through the throttle and the amount of mass flow the surge valve can recycle. The drawback is the need for sensitive and fast mass flow sensors, that are not an option today.

References

[1] Per Andersson. *Air Charge Estiamtion in Turbocharged Spark Ignition Engine*. Phd thesis 989, Department of Electrical Engineering, Linköpings Universitet, Linköping, Sweden, 2005.

[2] Björnar Böhagen and Jan Tommy Gravdahl. On active surge control of compressors using a mass flow observer. In *Proceedings for the 41th IEEE Conference on Decision and Control*, pages 3684–3689, Department of Engineering Cybernetics, Norwegian University of Science and Technology, NTNU-7491 Trondheim, Norway, 2002.

[3] Bram de Jager. Rotation stall and surge control: A survey. In *Proceedings of the 34th Conference on Decision and Control*, page 1587, December 1995.

[4] Bram de Jager and Frank Willems. Modeling and control of compressor flow instabilites. In *Control Systems Magazine, IEEE*, volume 19, pages 8–18, October 1999.

[5] Lars Eriksson. Modeling and control of turbocharged si and di engines. In *E-COSM - Rencountres Scientifiques de l'IFP*, volume 2, pages 21–34, October 2006.

[6] Lars Eriksson and Lars Nielsen. *Vehicular Systems*. Bokakademin Linköping, 2005. Course Material in Vehicular Systems.

[7] Olof Erlandsson. *Thermodynamic Simulation of HCCI Engine Systems*. Phd thesis, Department of Heat and Power Engineering, Lund Institute of Technology, Lund, Sweden, 2002. ISBN 91-628-5427-5.

[8] Jan Tommy Gravdahl. *Modeling and Control of Surge and Rotating Stall in Compressors*. Report 98-6-w, Department of Engineering Cybernetics, Norwegian University of Science and Technology, Department of Engineering Cybernetics, Norwegian University of Science and Technology, N-7034 Trondheim, Norway, 1998.

[9] Jan Tommy Gravdahl and Olav Egeland. Speed and surge control for a low order centrifugal compressor model. In *Proceedings of the 1997*

IEEE International Conference on Control Applications, page 344, Department of Engineering Cybernetics, Norwegian University of Science and Technology, N-7034 Trondheim, Norway, 1997.

[10] Jan Tommy Gravdahl, Olav Egeland, and Svein Ove Vatland. Active surge control of centrifugal compressors using drive torque. In *Proceedings for the 40th IEEE Conference on Decision and Control*, pages 1286–1291, Department of Engineering Cybernetics, Norwegian University of Science and Technology, NTNU-7491 Trondheim, Norway, 2001.

[11] E.M. Greitzer. The stability of pumping systems. *Journal of Fluids Engineering, Transactions of the ASME*, 103:193–242, June 1981.

[12] SAE International. Turbocharger gas stand test code. Not published, 4 1989. Reaffirmed 1995-03.

[13] G. Theotokatos and N. P. Kyratos. Diesel engine transient operation with turbocharger compressor surging. *SAE International*, March 2001.

[14] Wikipedia. `http://en.wikipedia.org/`, 2007. Downloaded 2007-05-29.

[15] E. Wiklund and C. Forssman. Bypass valve modeling and surge control for turbocharged si engines. Master's thesis LiTH-ISY-EX-3712, Department of Electrical Engineering, Linköpings Universitet, Linköping, Sweden, August 2005.

Appendix A

Simulink model implementations

This thesis uses three different Simulink models. A brief description of these three is given in this appendix.

A.1 Original MVEM model with non surge capable compressor

A non surge capable MVEM model was provided for the thesis. This model is developed in the Ph.D. thesis written by Per Andersson [1]. This original MVEM model is parameterized to behave like the turbocharged SI engine mounted in the engine lab at Vehicular Systems, ISY, Linköpings Universitet. This model uses sub models from the mean value engine modeling Simulink library MVEM_lib. This library consists of standard engine components (throttle, cylinders, exhaust manifold etc.). These components can be connected using control volumes in between. The original MVEM model uses some simplifications that need development for this thesis. The most important limitations are

- All compressor and intercooler flows run in forward direction.

- No surge valve is introduced since the test lab engine originally lacked one.

- No surge capability.

These limitations are handled by extending the provided MVEM model as described in the next section. Figure A.1 shows an overview of the Simulink implementation. For more detailed information about this model and MVEM in general see [1].

A.2   Developed MVEM model with surge capabilities

For the original MVEM model described in the previous section to be useful, it needs to be expanded with a surge valve and surge handling capability. The surge valve is described in section 4.2.1. During surge the mass flow is reversed. In this developed MVEM model it is assumed that this only needs to be modeled between the closest control volumes upstream and downstream of the compressor. A better model would incorporate reversed mass flow capability even further downstream of the compressor. An overview of the developed MVEM model with a surge valve and flow reversal capability is shown in figure A.2. For a more detailed view of the compressor model connections and the sub models making up the compressor model see figure A.4. Apart from the changes described the developed, this MVEM model is a copy of the original MVEM model.

A.3   Surge test rig model

Some of the available data are measured in a surge test rig. To be able to simulate and validate different compressor sub models against this data a Simulink model is constructed to imitate the test rig. This Simulink model has much lower complexity than the full MVEM engine models. This is because the surge test rig uses a constant shaft speed. The compressor is powered by a separate electric/hydraulic engine. This Simulink model does not have a surge valve because this is never used in the supplied data sets. In the Simulink model different inputs can be chosen depending what to study. An overview of the surge test rig Simulink model is shown in figure A.3. The different sub models making up the compressor model are shown in figure A.4.
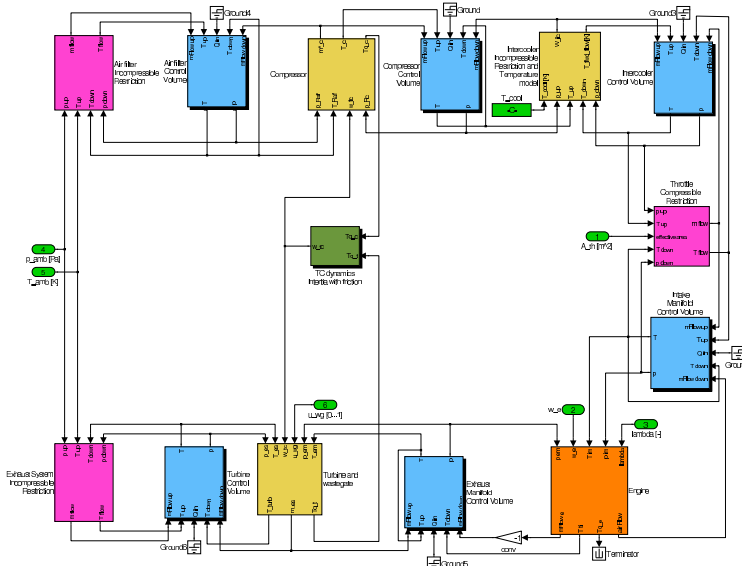
Figure A.1: Original MVEM SI engine model without surge capability.
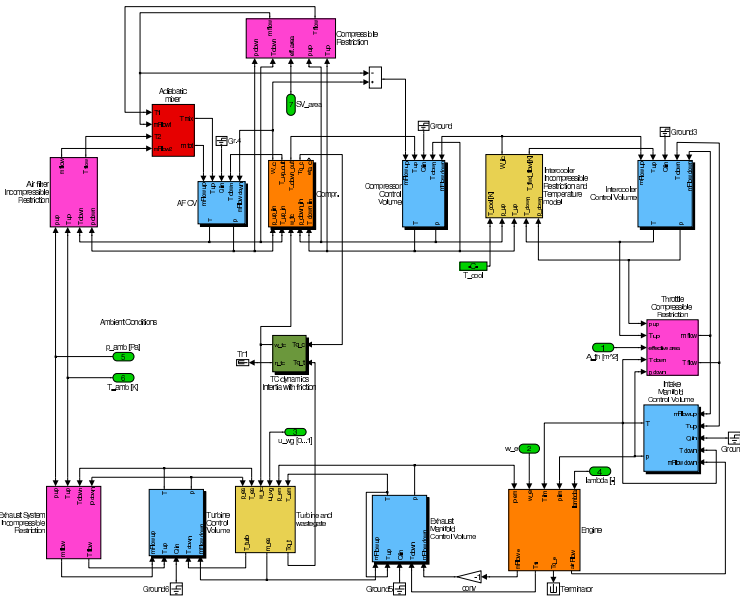

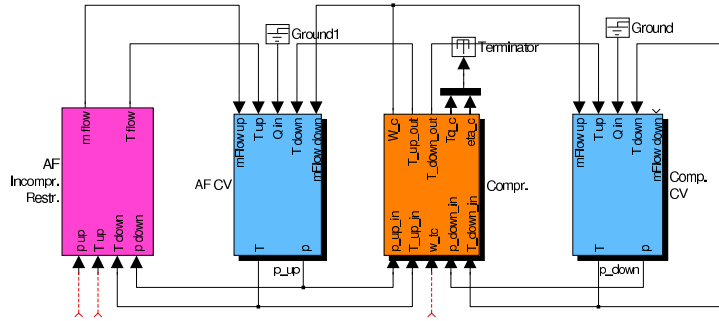Figure A.2: The extended Simulink model capable of modeling surge.

Figure A.3: An overview of the surge test rig Simulink model.
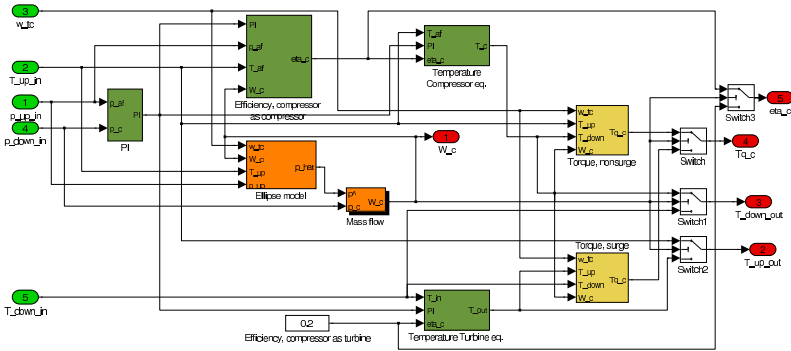

Figure A.4: A detailed view of the compressor model sub models. The important sub models are the efficiency as compressor, temperature as compressor, torque as compressor, the pressure build up and the Ellipse model.

Appendix B

Nomenclature

Listed here are the variables and their subscripts used in the thesis. A short example: W_c. W means mass flow, c means compressor. $W_c = Compressor\ mass\ flow$.

Variable	Parameter	Unit
δ	Normalizing factor	—
γ	Ratio of specific heats	—
η	Efficiency	—
Φ	Normalized air mass flow	—
Θ	Normalizing factor	—
Ψ	Head parameter	—
A	Valve area	m^2
c_p	Specific heat constant	—
D	Inlet diameter	m
J	Shaft inertia	N
L	Duct length	m
N	Rotational speed	rpm
m	Mass	kg
Π	Pressure ratio	—
$\hat{\Pi}$	Pressure build up ratio	—
p	Pressure	Pa
Q	Estimate matrix elements	—
R	Specific gas constant	—
T	Temperature	K
t	Time	s
Tq	Torque	Nm
U	Impeller tip speed	$\frac{m}{s}$
w	Rotational speed	$\frac{rad}{s}$
W	Mass flow	$\frac{kg}{s}$
ΔW	Mass flow difference	$\frac{kg}{s}$

Subscript	Name
af	Air filter
amb	Ambient
c	Compressor
$corr$	Corrected
$crit$	Critical
eff	Effective
$high$	High
im	Intake manifold
$init$	Initial
low	Low
max	Maximum
$mergedCV$	Merged control volume
$mixed$	Mixed
$needed$	Needed
ref	Reference
std	Standard
$surge$	At surge line or to surge line
sv	Surge valve
t	Turbine
tc	Turbocharger
th	Throttle
tot	Total

Copyright

Svenska

Detta dokument hålls tillgängligt på Internet - eller dess framtida ersättare - under en längre tid från publiceringsdatum under förutsättning att inga extraordinära omständigheter uppstår.

Tillgång till dokumentet innebär tillstånd för var och en att läsa, ladda ner, skriva ut enstaka kopior för enskilt bruk och att använda det oförändrat för ickekommersiell forskning och för undervisning. Överföring av upphovsrätten vid en senare tidpunkt kan inte upphäva detta tillstånd. All annan användning av dokumentet kräver upphovsmannens medgivande. För att garantera äktheten, säkerheten och tillgängligheten finns det lösningar av teknisk och administrativ art.

Upphovsmannens ideella rätt innefattar rätt att bli nämnd som upphovsman i den omfattning som god sed kräver vid användning av dokumentet på ovan beskrivna sätt samt skydd mot att dokumentet ändras eller presenteras i sådan form eller i sådant sammanhang som är kränkande för upphovsmannens litterära eller konstnärliga anseende eller egenart.

För ytterligare information om Linköping University Electronic Press se förlagets hemsida: `http://www.ep.liu.se/`

English

The publishers will keep this document online on the Internet - or its possible replacement - for a considerable time from the date of publication barring exceptional circumstances.

The online availability of the document implies a permanent permission for anyone to read, to download, to print out single copies for your own use and to use it unchanged for any non-commercial research and educational purpose. Subsequent transfers of copyright cannot revoke this permission. All other uses of the document are conditional on the consent of the copyright owner. The publisher has taken technical and administrative measures to assure authenticity, security and accessibility.

According to intellectual property law the author has the right to be mentioned when his/her work is accessed as described above and to be protected against infringement.

For additional information about the Linköping University Electronic Press and its procedures for publication and for assurance of document integrity, please refer to its WWW home page: `http://www.ep.liu.se/`